Viscoelastic Analysis Applied to the Determination of Long-Term Creep Behavior for Magnetic Tape Materials

Brian L. Weick

Mechanical Engineering Department, School of Engineering and Computer Science, University of the Pacific, Stockton, California 95211

Received 28 October 2005; accepted 27 February 2006
DOI 10.1002/app.24341
Published online in Wiley InterScience (www.interscience.wiley.com).

ABSTRACT: Creep-compliance experiments were performed for three representative magnetic tapes. Two of these tapes used a magnetic particle (MP) coating, and one used a metal-evaporated (ME) coating. The MP tapes used the following polyester substrates: semitensilized poly(ethylene naphthalate) (PEN) and supertensilized poly(ethylene terephthalate). The ME tape used an aromatic poly(amide) or aramid substrate. Time–temperature superposition was used to make creep-compliance predictions at 30 and 50°C reference temperatures. Comparisons were made with dimensional stability requirements based on position error signal (PES) specifications for magnetic tape drives along with in-cartridge creep specifications based on PES measurements. Circumferential and lateral creep strains were determined that account for storage of the tapes in a reel, and creep strains were predicted for future tapes with thinner, lower compliance coatings. A rule of mixtures method was also used to extract compliance information for individual layers of MP-PEN tapes, and stress profiles through the thickness of the tapes were determined. Additional measurements and analyses were performed to determine the creep recovery and shrinkage characteristics for the magnetic tapes. © 2006 Wiley Periodicals, Inc. J Appl Polym Sci 102: 1106–1128, 2006

Key words: creep; polyesters; viscoelastic properties; magnetic tapes; PES

INTRODUCTION

Magnetic tape continues to be a key player in long-term storage applications required by business and government.[1] Advances continue to be made in tape drives as well as magnetic tape materials, and projections for future tape cartridges call for substantial improvements in media dimensional stability due to the increase in the number of tracks per inch.[1] One format, the Linear Tape Open or LTO format, calls for a half inch tape cartridge to hold 800 GB with 1024 data tracks by 2008. The LTO format was developed by multiple technology provider companies as a general mid-range tape format. As an example of the kind of improvements made during the past few years, the first 100 GB LTO generation tape became available in 2000 and held 384 tracks, which was a substantial improvement over other mid-range linear tapes at that time. In 2002, the 200 GB LTO Generation 2 cartridges became available with 768 tracks, and 400 GB Generation 3 cartridges became available in 2004 with the same number of tracks, but other improvements were made to increase the capacity of the tape.[2]

Thickness reduction of the magnetic tape is one method that tape manufacturers intend to use to achieve higher storage capacities. This reduction can be in the magnetic layer, or in the substrate, or both. Relatively thick magnetic layers comprised of dispersed magnetic particles (MP) in a polymeric binder are used in LTO and digital linear tape (DLT), and improvements in these layers could increase storage capacity. In comparison, ultra-thin metal-evaporated (ME) magnetic layers are used in advanced intelligent tapes (AIT) to achieve high storage capacities in an 8-mm-wide tape. Alternative substrates could also be developed to replace the current polyester substrates that dominate the magnetic tape industry, and polymer film manufacturers have found ways to improve the mechanical and viscoelastic characteristics of the polyesters through processes such as tensilization. Aromatic polyamides or aramid substrates have begun to see more use for magnetic tapes such as AIT, but their high cost still inhibits their use in many applications.

Mechanical and viscoelastic characteristics of alternative substrates for magnetic tape materials have been studied by Weick and Bhushan,[3] and they used analytical approaches to study the characteristics of magnetic tape layers.[4,5] Creep experiments discussed in these studies were performed at elevated temperatures, and time–temperature superposition (TTS) was used to predict long-term behavior. Creep strains and

Correspondence to: B. L. Weick (bweick@pacific.edu).
Contract grant sponsor: Information Storage Industry Consortium (INSIC).

TABLE I
Magnetic Tape Specifications

	MP-PEN	MP-PET	ME-Aramid
Tape Manufacturer and Trade Name	IBM Total Storage LTO Generation 2 Ultrium Data Cartridge	Quantum Super DLT tape II Media	Sony AIT-3 Tape Cartridge
Native capacity (GB)	200	300	100
Compressed capacity (GB)	400	600	260
Tape width (mm)	12.7	12.7	8
Nominal tape thickness (μm)	8.9	8.0	5.3
Substrate material	poly(ethylene naphthalate) (PEN): semi-tensilized	poly(ethylene terephthalate) (PET): super-tensilized	Aramid: aromatic polyamide
Nominal substrate thickness (μm)	6.5	–	4.5
Magnetic layer	Magnetic particle (MP)	Magnetic particle (MP)	Metal-evaporated (ME)

lateral contractions were predicted for tapes and substrates in use during the late 1990s, accounting for storage of the magnetic tape in a reel.[5] Additional work by Higashioji and Bhushan[6] studied characteristics of commercial tensilized polyester substrates, and Ma and Bhushan[7] studied the creep characteristics of magnetic tapes and substrates subjected to elevated humidity.

Although some qualitative connections were made between creep measurements performed in the lab and tape failure mechanisms, more studies were needed to develop improved measurement techniques and standards that correlate viscoelastic characteristics measured during creep experiments with dimensional stability requirements for current and future magnetic tapes. On the basis of this need, one objective of this research was to perform creep experiments using representative magnetic tape materials used for current mid-range recording applications. These materials are summarized in Table I, and consist of two MP tapes with poly(ethylene naphthalate) (PEN) and poly(ethylene terephthalate) (PET) substrates as well as a ME tape with an aramid substrate. Additional objectives include using analytical techniques developed in past research such as the rule-of-mixtures[4,5] method to extract creep characteristics of magnetic layers, and the standard TTS process for predicting long-term creep behavior.[3,5] It was also an objective of this research to refine a reel model to predict creep strain and assist with the prediction of lateral creep strains in magnetic tapes during storage. Quantitative correlations between the experimental creep measurements and lateral stability requirements for current and future magnetic tapes could then be performed as a final objective.

EXPERIMENTAL CREEP TESTING

Overview

The experimental procedure for creep testing follows similar practices developed and discussed by Weick and Bhushan.[3,5] Summaries of the test equipment and experimental procedure can be found in their past work,[3–5] and these summaries have been rewritten and edited in light of the methodology used for the research presented herein.

Test equipment

Creep-compliance measurements were made using the apparatus shown in Figure 1, which was developed by Bhushan[8,9] and Weick and Bhushan.[3] The magnetic tape specimens were tested simultaneously using this apparatus, which was placed in an incubator at the prescribed test temperature. The apparatus

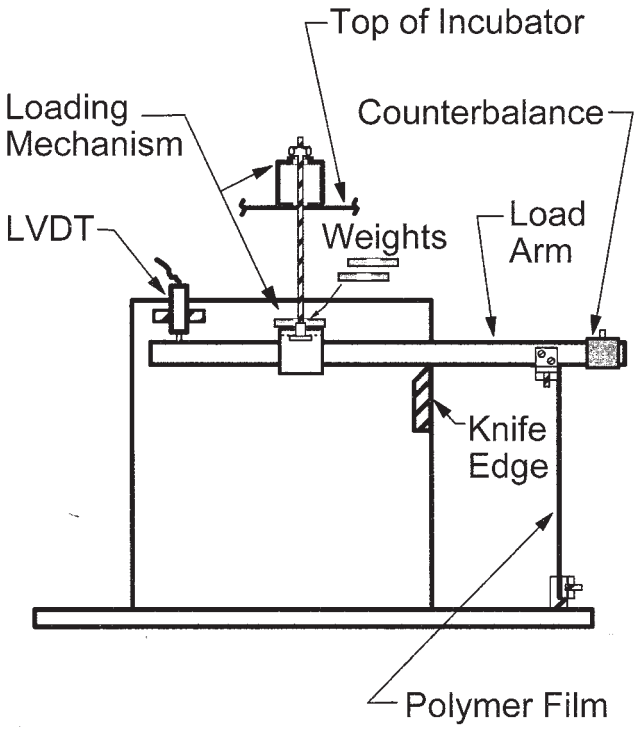

Figure 1 Schematic view of a creep tester for evaluating the creep behavior of magnetic tape materials.

consisted of four balance beams (or load arms), and the test specimens were fixed at the end of each balance beam and aligned with a straight-edge. A linear variable differential transformer (LVDT) was connected to the other end to measure deflection of the load arm due to creep of the test specimen, and the LVDT output was recorded on a PC. As shown in Figure 1, weights were placed on top of support pieces positioned around each load arm. Lowering or raising the support pieces was done remotely using a hand-driven lead screw mechanism after the incubator reached the preset test temperature.

Determination of creep-compliance

During an experiment the LVDT connected to each load arm measures the change in length of each magnetic tape test specimen. This change in length is in general a nonlinear function of time (and temperature) for polymers. The amount of strain the test specimen is subjected to can be calculated by normalizing the change in length of the specimen with respect to the original length. Creep-compliance can then be calculated by dividing the time-dependent strain by the constant applied stress:

$$\varepsilon(t) = \frac{\Delta l(t)}{l_o} \tag{1}$$

$$D(t) = \frac{\varepsilon(t)}{\sigma_o} = \frac{\Delta l(t)}{\sigma_o l_o} \tag{2}$$

where $\Delta l(t)$ is the change in length of the test specimen as a function of time, l_o is the original length of the test specimen, $\varepsilon(t)$ is the amount of strain the film is subjected to, σ_o is the constant applied stress, and $D(t)$ is the tensile creep-compliance of the test specimen as a function of time.

Creep-compliance data for the test specimens are modeled using a generalized Kelvin-Voigt model, which has the following mathematical form:

$$D(t) = D_o + \sum_{k=1}^{K} D_k[1 - \exp(-t/\tau_k)] \tag{3}$$

where D_o is the instantaneous compliance at time $t = 0$, D_k is the discrete compliance terms for each Kelvin-Voigt element, and τ_k is the discrete retardation times for each Kelvin-Voigt element.

Based on this model, for a constant stress of magnitude σ_o applied at $t = 0$, the instantaneous response of a viscoelastic solid will be a sudden strain of magnitude $\varepsilon_o = \sigma_o D_o$. This is followed by a delayed (or retarded) response, which can be attributed to the additional exponential terms in eq. (3). More specifically, each kth element of the model contributes a delayed compliance of magnitude D_k [$1 - \exp(-t/\tau_k)$], and the amount of this delay is directly related to the magnitude of the retardation times τ_k.[10,11]

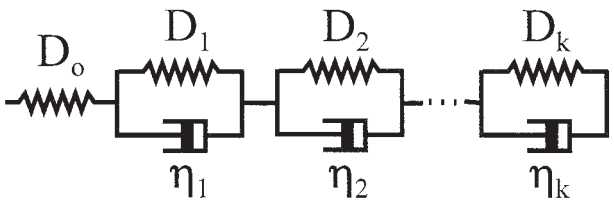

Figure 2 The Kelvin-Voigt model used to express the elastic and viscous characteristics of polymeric materials.

Equation (3) is typically represented as a series of parallel springs and dashpots connected to a single spring. This mechanical analog is shown in Figure 2, and is indicative of a viscoelastic polymer, which has an amorphous phase with mainly unoriented molecules, and a crystalline phase, which contains oriented molecules. Components of the polymeric structure, which respond instantly to an applied stress, are modeled as a single spring with an instantaneous compliance D_o. Components of the polymeric structure, which do not respond instantly but are deformed in a time-dependent manner, are modeled as multiple elements consisting of springs and dashpots acting in parallel. Each element contains a spring, which has a compliance D_k, and a dashpot with a viscosity equal to η_k. The retardation time for each kth element is defined below:

$$\tau_k = \eta_k D_k \tag{4}$$

Note that the retardation time can also be interpreted as the length of time required to attain $(1 - 1/e)$ or 63.2% of the equilibrium strain for each element.[9,10–12]

Experimental data sets are fitted to eq. (3) using a nonlinear least-squares technique known as the Levenberg-Marquardt method.[13] This method is used to find the best-fit parameters τ_k and D_k for a Kelvin-Voigt model with multiple elements. Previous work by Weick and Bhushan[3,5] to determine the viscoelastic characteristics of alternative polymeric substrates used for magnetic tapes showed that two to three elements are typically required for a reasonable fit.

Experimental procedure for performing creep experiments

Prior to loading the samples, the incubator was turned on to stabilize the temperature in the chamber and allow the structure of the creep tester to undergo any dimensional changes. During this stabilization period of typically 3 h, the signals from the LVDT's were monitored until they were steady. At this point the

chamber was opened and the samples were fastened between the load arms and base of the creep tester. A preload of 0.5 MPa was applied to the specimens by adjusting the counterbalance weight on the load arm. The chamber was then closed and changes in length of the samples were monitored for 10 h to account for any additional expansion of the test apparatus, and account for shrinkage of the samples. After the 10 h period at 0.5 MPa, an additional 6.5 MPa stress was applied to the specimens using the external control mechanism for a total applied stress of 7.0 MPa. This relatively low stress has been shown to keep the creep experiments in the linear viscoelastic regime.[3,9] For the first hour, the sampling rate for the 16 bit data acquisition system was set to 1 sample/s per load arm. After 1 h, the sampling rate was slowed down to 1 sample every 100 s. Creep characteristics of the specimens were monitored for at least an additional 49 h, with longer time periods being used at 70°C. At the end of the creep experiment, the sampling rate was once again increased to 1 sample/s per load arm, and the specimens were unloaded. Recovery characteristics were then monitored at the lower sampling rate for approximately 10 h or until the signals reached a steady level. All creep experiments discussed herein were performed at 30, 50, or 70°C. Humidity was uncontrolled during the experiments, but was measured to be 25–30% during the 30°C experiments, less than 10% during the 50°C experiments, and 0% during the 70°C experiments.

Test specimens

Magnetic tapes selected for this study are described in Table I. The MP-PEN and MP-PET tapes are particulate tapes consisting of front coats with magnetic and nonmagnetic layers coated on to a substrate, with thin back coats applied to the substrate. The front coats are composed of MPs dispersed in a polymeric binder deposited on a nonmagnetic coating. Typical MP coatings for Fuji tapes consist of Fe metal alloy particles suspended in a polymeric binder consisting of vinylchloride copolymer, polyurethane, and polyisocyanate as a hardener.[5] Specific formulations for the MP tapes used in this study are proprietary. The magnetic and nonmagnetic front coats are deposited on to polyester substrates. PEN is used for MP-PEN, and PET is used for MP-PET. Back coats for the MP-tapes are typically organic polymers, and nitrocellulose is a common back coat material.[5]

Properties and characteristics of polyester substrates (PET and PEN) have been well-documented by Bhushan[8,9] and Weick and Bhushan[3–5] along with the properties of aramid substrates. PET used in MP tapes is typically tensilized for a high Young's modulus in the machine direction.[6] The glass transition temperature for PET is typically 78°C, with the glass transition temperature for PEN reported as being somewhat higher (156°C).[3] These glass transition temperatures represent the primary temperatures at which large scale specific volume and elastic modulus changes begin to occur in polymers as they are heated-up from room temperature. The macromolecules in the amorphous regions of the polymers are no longer "frozen" in place above the glass transition temperature and are capable of short to long range motion, but molecules in the crystalline region do not begin to move until the crystalline melting point is reached. It is important to note that additional transition or relaxations can also occur in polyester substrates because of other secondary motions of molecular groups in the polymers. These secondary relaxations tend to appear in polyester creep data at elevated temperatures below the glass transition point, and are predicted to occur at room temperature after extended time periods.[3,5]

The ME-Aramid tape used in this study is composed of a ME continuous film of magnetic materials deposited on to the aromatic polyamide (aramid) substrate using vacuum techniques. A back coat is applied to the ME-Aramid substrate to complete the tape. Although specific information about the front coat is not available for proprietary reasons, the continuous ME coating for ME tapes is typically a dual layer of evaporated Co-O.[5]

LONG-TERM CREEP-COMPLIANCE CHARACTERISTICS

Methodology

TTS has been used in past research to predict long-term creep behavior at ambient temperature.[11,14] This analytical technique uses creep measurements at elevated temperature levels to predict behavior at longer time periods. In this research, data sets acquired at 30, 50, and 70°C are superimposed at a reference temperature of 30°C to determine long-term creep behavior over an extended time period. The rationale for this methodology stems from the observation that most polymers will behave in the same compliant manner at a particular high temperature as they will when they are deformed at a particular slow rate at room temperature. This means that there is a correspondence between time (or rate of deformation) and temperature.

Results and discussion

Initial compliance values from experimental data

Three repeat experiments were performed at each of the 30, 50, and 70°C temperature levels to determine variability in the data sets. Figure 3 shows raw data sets acquired at 50°C for MP-PEN, MP-PET, and ME-Aramid tapes, and three data sets are shown for each

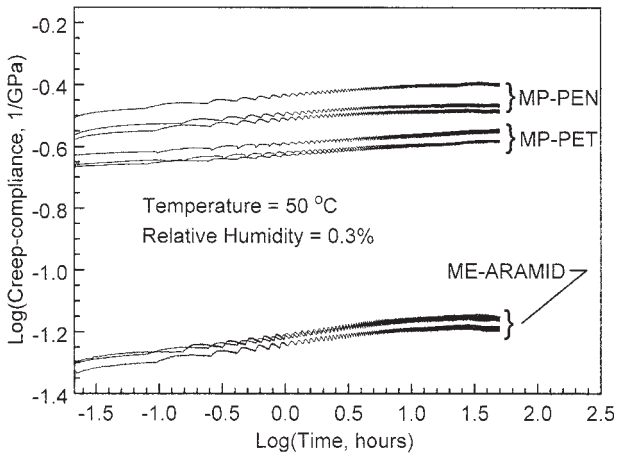

Figure 3 Creep-compliance data for MP-PEN, MP-PET, and ME-Aramid tapes. Data sets are from three repeat experiments performed for each tape.

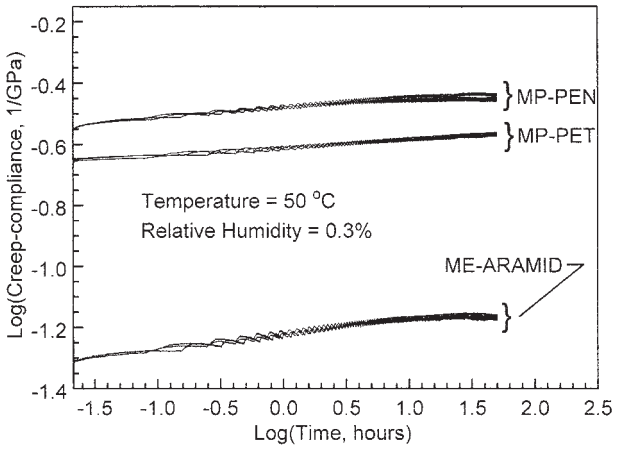

Figure 4 Creep-compliance data for MP-PEN, MP-PET, and ME-Aramid tapes after using an average initial creep-compliance value (D_o) to adjust for variance in the initial loading.

tape type. Each data set has a small band of noise associated with the experimental process, but there is also some variation between the three repeat experiments. This variation can be attributed to the hand-driven loading mechanism that is used to place the weights on the load arm. This causes variations in the initial loads on the magnetic tapes, which shows-up as variations in the initial creep-compliance, D_o. Using initial creep-compliance values for each of the three repeat experiments, an average initial creep-compliance was determined for each tape and temperature level. Table II provides a summary of these average creep-compliances along with standard deviations. By utilizing the average creep-compliance, the variation between the repeat experiments is removed. Figure 4 provides an example of how average creep-compliances determined using repeat experiments were used to remove the variation from the data sets acquired at 50°C. Average log(D_o) values of −0.549, −0.649, and −1.310 were used for these plots as shown in Table II for MP-PEN, MP-PET, and ME-Aramid, respectively. These log(D_o) values correspond with D_o values of 0.282, 0.224, and 0.049 GPa^{-1} when the inverse logarithms are calculated. Note that base 10 logarithms of the creep-compliance in GPa^{-1} and time in hours were used for all plots, which simplifies the tick marks and labels for the figures.

TABLE II
Average Initial Creep-Compliance Values (D_o) and Standard Deviations Calculated Using Three Repeat Experiments. (Average Initial Values Calculated 20 s After Start of Loading Period.)

	Log (Initial creep-compliance (D_o) 1/GPa)		
	MP-PEN	MP-PET	ME-Aramid
30°C			
Average	−0.575	−0.681	−1.270
Standard deviation	0.070	0.036	0.203
50°C			
Average	−0.549	−0.649	−1.310
Standard deviation	0.037	0.017	0.020
70°C			
Average	−0.512	−0.654	−1.180
Standard deviation	0.075	0.043	0.104

Creep-compliance data at 30, 50, and 70°C

Figures 5–7 show raw data acquired for the MP-PEN, MP-PET, and ME-Aramid tapes, respectively. Average initial creep-compliance (D_o) values shown in Table II were used to adjust for variance in initial loading, which enabled the repeatability of the experiments to be clearly shown in the figures. Some variability was observed at the end of the 30°C experiments, but this can be attributed to room temperature changes that caused larger temperature shifts in the incubator. Experiments at 50°C showed minimal variability after adjusting the data sets using average initial creep-compliance values. The 70°C experiments also showed minimal variability after adjustment using the average D_o values. Note that two of the three 70°C repeat experiments were performed for over 100 h, and the third repeat experiment was only performed for 1 h. The extended 70°C experiments enabled longer time predictions after TTS.

To enable further analysis, the raw data sets were fitted to the Kelvin-Voigt model. Representative data sets were chosen from those shown in Figures 5–7, and the best fit parameters τ_k and D_k were determined using the Levenberg-Marquardt algorithm for multiple Kelvin-Voigt elements shown in eq. (3) and Figure 2. Typically, two elements were needed for the 30°C

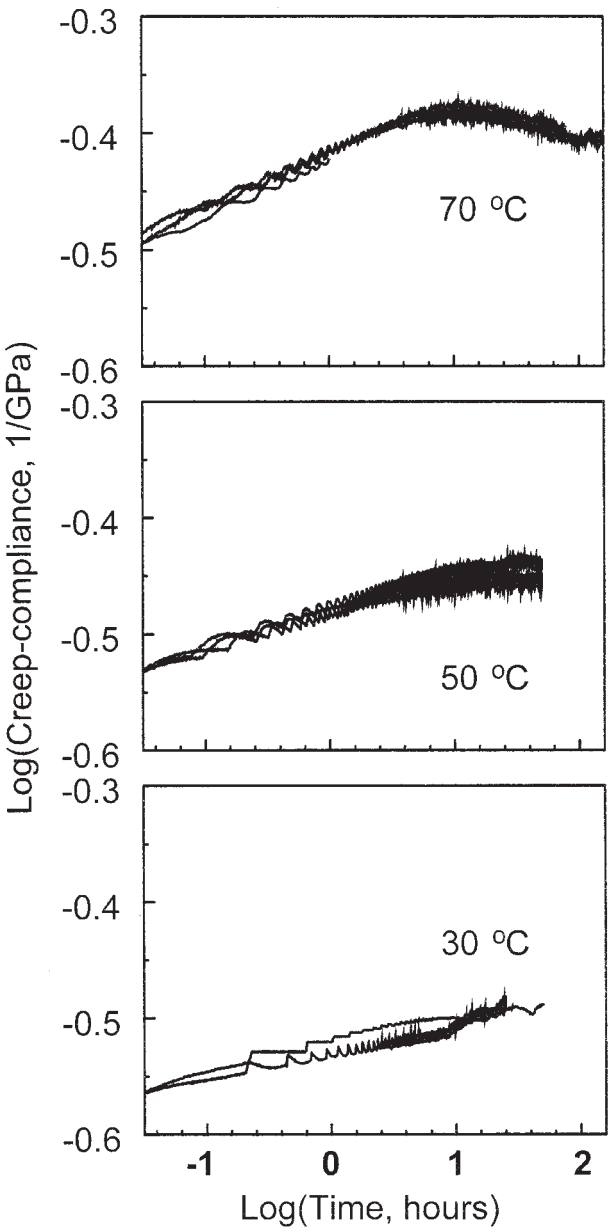

Figure 5 Experimental creep-compliance data at 30, 50, and 70°C for MP-PEN tape. An initial average creep-compliance value (D_o) is used to adjust for variance in the initial loading, and repeat experiments are shown.

data, and three elements were needed for the 50 and 70°C data. This is in keeping with past research on magnetic tapes and substrates that used the Kelvin-Voigt viscoelastic model. Figure 8 shows the resulting curve fits for the MP-PEN, MP-PET, and ME-Aramid tapes. Note that data shown in Figure 8 for the MP-PEN tape represent curve fits for the data sets shown in Figure 5. Similarly, data shown in Figure 8 for the MP-PET and ME-Aramid tapes represent curve fits for the data sets shown in Figures 6 and 7.

Upon examination of the creep-compliance data for the MP-PEN and MP-PET tapes with polyester substrates and similar magnetic coatings, it is interesting to note the clear separation between the creep behavior at 30, 50, and 70°C. For MP-PEN, the overall creep behavior at 30°C is relatively low, and increases in increments at 50 and 70°C. The slope of the creep-compliance curves indicates rate of creep, and this appears to be similar at all temperatures for MP-PEN during the initial part of the experiment. However, at 70°C and toward the end of the 50°C experiment, the creep-compliance curves level-off and actually start to decrease for MP-PEN. This could indicate that a transition point had been reached for the MP-PEN tape. Creep-compliance results for MP-PET show an overall

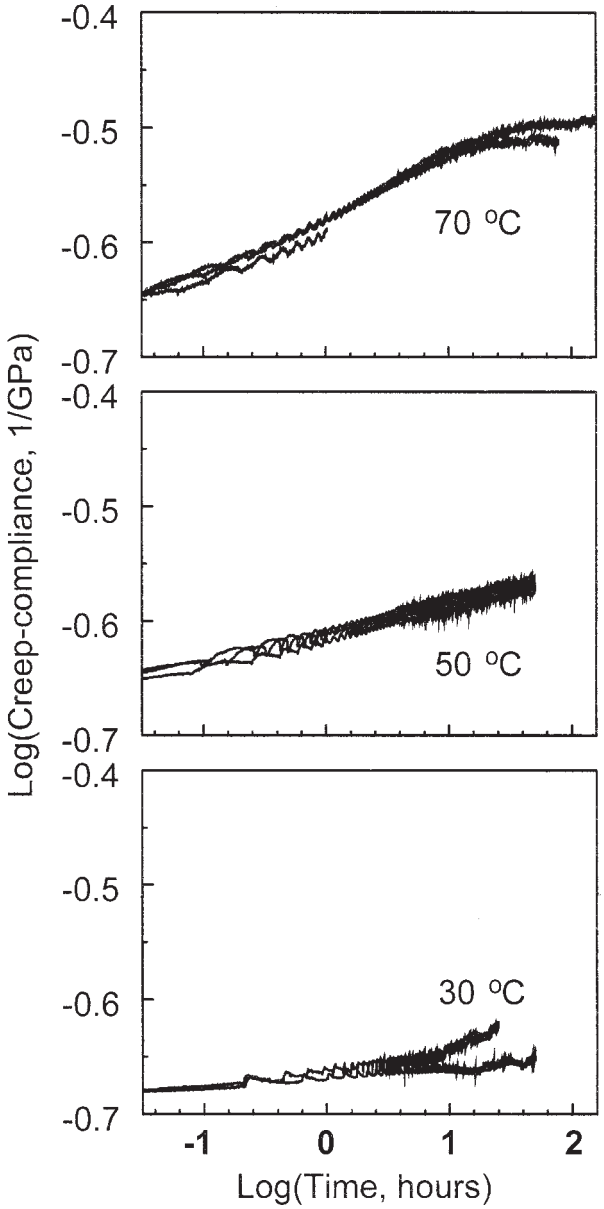

Figure 6 Experimental creep-compliance data at 30, 50, and 70°C for MP-PET tape. An initial average creep-compliance value (D_o) is used to adjust for variance in the initial loading, and repeat experiments are shown.

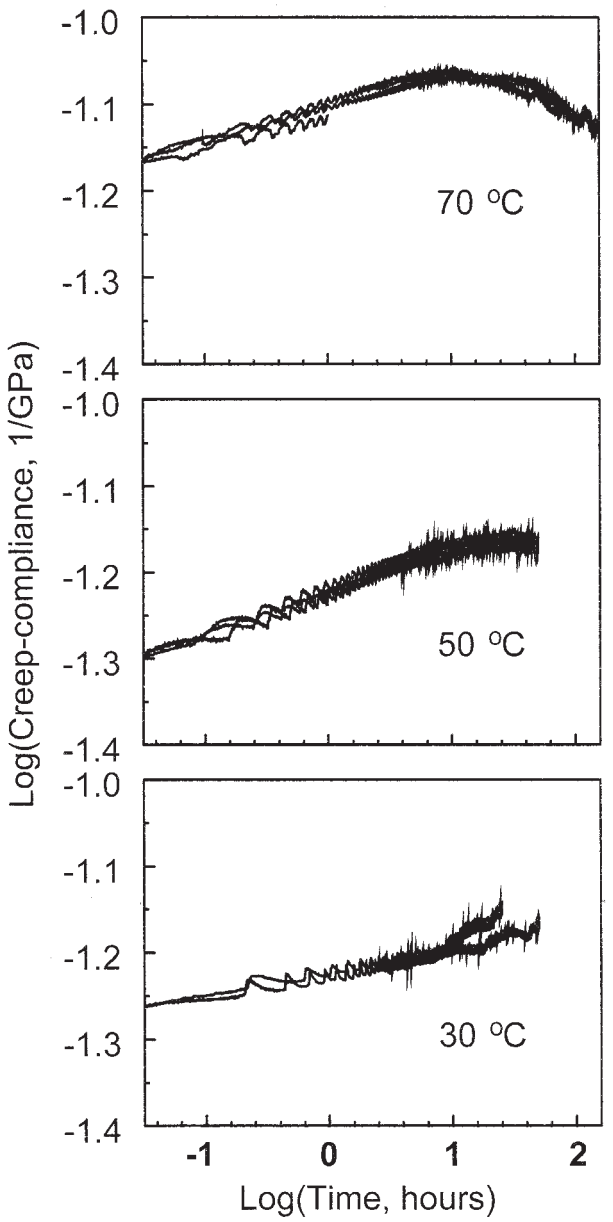

Figure 7 Experimental creep-compliance data at 30, 50, and 70°C for ME-Aramid tape. An initial average creep-compliance value (D_o) is used to adjust for variance in the initial loading, and repeat experiments are shown.

creep behavior that is lower than what was measured for MP-PEN. As observed for MP-PEN, the overall creep behavior is lowest at 30°C and higher at the elevated temperatures for MP-PET. However, the creep rate for the MP-PET tape appears to change significantly as temperature is increased from 30 to 50 to 70°C. A peak is also observed for MP-PET at 70°C after approximately 10 h, although this appears to be shifted to the right when compared with MP-PEN and does not lead to the same decrease in creep-compliance.

The ME-Aramid tape exhibits an overall creep-compliance that is lower than the compliance for the tapes with polyester substrates. The 50°C creep-compliance curve starts off at a lower initial compliance value than the 30°C curve; however, the slope of the 50°C curve is greater. Creep behavior at 70°C exhibits a higher overall creep than what was observed for the 30 and 50°C experiments. In addition, the creep-compliance for the ME-Aramid material also appears to exhibit a peak and plateau at 70°C followed by a decrease in creep-compliance. Once again, this could be due to transitions in the tape materials caused by the stress applied to the tape at the elevated temperature over an extended time period.

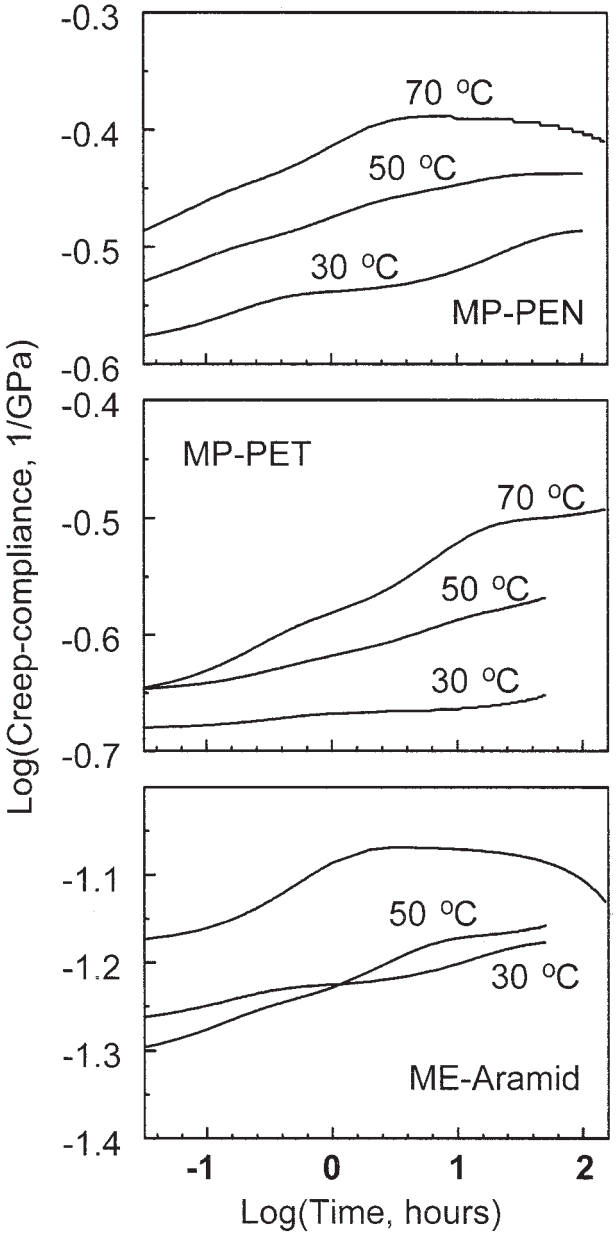

Figure 8 Creep-compliance curves after fitting data to the Kelvin-Voigt viscoelastic model. Curve fits are shown for MP-PEN, MP-PET, and ME-Aramid at 30, 50, and 70°C.

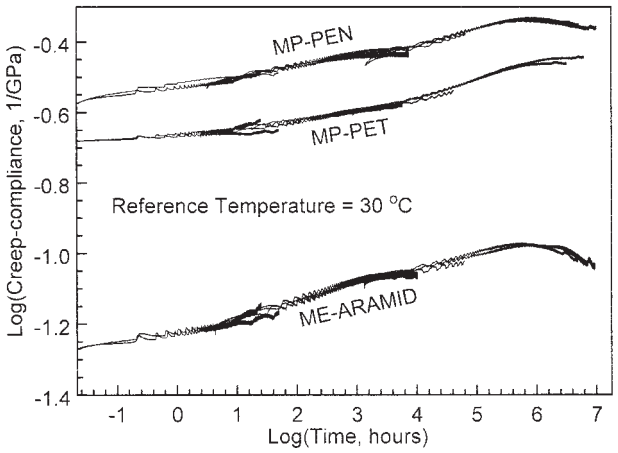

Figure 9 Creep-compliance master curves for magnetic tape materials after TTS of experimental data acquired at three temperature levels.

Creep-compliance master curves at 30°C

The raw data sets shown in Figures 5–7 are superimposed on each other using the TTS process to produce the master curves shown in Figure 9. A reference temperature of 30°C is used for this superposition process, which allows for long-term creep-compliance to be predicted out to time periods as long as 10^7 h. Curve fits shown in Figure 8 can also be used to generate TTS curves shown in Figure 10. These continuous plots enable future analyses to be performed with the data.

Overall, Figures 9 and 10 show that MP-PEN exhibits the greatest overall creep followed by MP-PET and ME-Aramid. Trends and transitions to the data plotted at 50 and 70°C after short periods of time show-up in the superimposed data at 30°C after a long period. As an example, from Figure 8, the peak shown in MP-PEN at 70°C after approximately 1 h will occur at 30°C after approximately 10^5 h based on the superimposed data shown in Figures 9 and 10. The peak in ME-Aramid also occurs after this extended time period at 30°C, with MP-PET exhibiting a peak without the same type of decrease after approximately 10^6 h.

Comparisons with position error signal measurements and specifications

Dimensional stability of magnetic tape materials can be measured after the tape is manufactured and stored in a reel. A type of signal known as the position error signal (PES) is used to make the measurements. PES can be defined as the residual error between a target position on the tape and the actual head position on the tape in the lateral direction.[1] (The lateral direction is across the width of the tape.) Position errors can occur due to media defects, or drive problems such as lateral tape motion, wear, etc.[1,2] A method for measuring the PES involves using two servo bands written on the tape to enable track following. This method calls for measuring the distance between the two servo bands down the length of the tape at room temperature and humidity. Then, the tape cartridge is placed in a 55°C, 40% relative humidity environment for 10 days. After that time period, the distance between the two servo bands is re-measured down the length of the tape. The maximum change in width of the tape is the tape width after the exposure to the elevated temperature and humidity minus the tape width at room temperature and humidity. This measurement is sometimes referred to as the "in-cartridge creep," and is a lateral measurement across the width of the tape.[1]

Creep-compliance measured in the research presented herein is along the length of the tape sample, and a Possion's ratio must be used to make comparisons with the in-cartridge creep from PES measurements. Assuming a Poisson's ratio of 0.3,[3,5,8,9] maximum lateral creep measurements can be determined using the TTS data shown in Figure 10. Recall that a 7.0 MPa nominal applied stress is used for the creep-compliance experiments and the calculations because it represents a typical drive tension used in tape drives. Using a creep-compliance value and this 7.0 MPa stress, eq. (2) can be solved for the longitudinal creep strain, $\varepsilon(t)$, and the lateral strain can be determined by multiplying this longitudinal strain by the Poisson's ratio. Note that this lateral strain represents a nominal strain for the magnetic tape when it is stored in a reel. Actual pack stresses and strains can

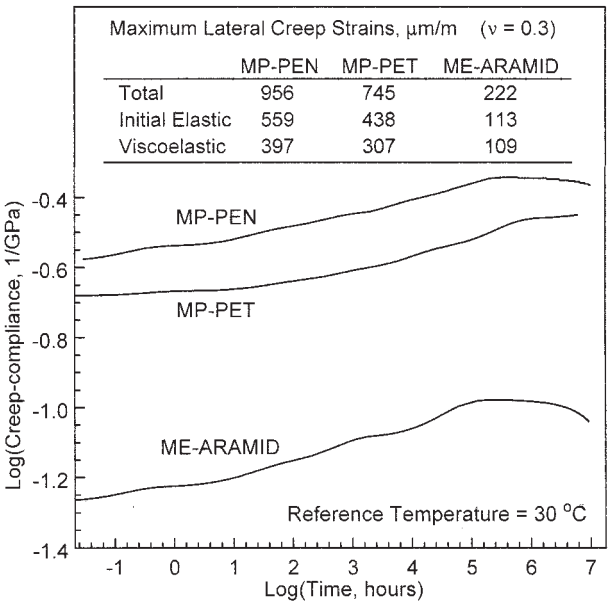

Figure 10 Creep-compliance master curves at a 30°C reference temperature using data sets fitted to the Kelvin-Voigt viscoelastic model. The master curves were generated using TTS of the curve fits for the magnetic tape materials at three temperature levels.

TABLE III
Dimensional Stability Parameters for Future Magnetic Tapes. These Requirements Show What Needs to be Achieved to Prevent Track Misregistration (International Magnetic Tape Storage Roadmap, 2005, p 82, © Information Storage Industry Consortium, adapted by permission.[1])

	2007	2009	2011	2013	2015
High bits per inch scenario					
Media written-in PES[a] (μm)	0.109	0.076	0.053	0.037	0.026
Media dimensional stability (μm/m)	1030	930	840	760	680
High tracks per inch scenario					
Media written-in PES[a] (μm)	0.101	0.067	0.044	0.029	0.019
Media dimensional stability (μm/m)	1000	890	790	700	620

[a] Position error signal (PES) is the residual error between a target position on the tape and the actual head position on the tape in the lateral direction.[1]

vary in a reel along with the associated dimensional stability, which can cause the tape to get wider or narrower depending on the location of a tape segment in the pack.

After the calculations are performed, the maximum total lateral creep strain for the MP-PEN, MP-PET, and ME-Aramid tapes is predicted to be 956, 745, and 222 μm/m, respectively, as shown in Figure 10. If the creep strain that corresponds with the initial elastic response (D_o) is subtracted from the total lateral creep, then the viscoelastic creep strain can be calculated. This viscoelastic creep is predicted to be 311, 128, and 105 μm/m for the MP-PEN, MP-PET, and ME-Aramid tapes. The Information Storage Industry Consortium (INSIC) has developed dimensional stability requirements for future magnetic tapes. Table III provides a summary of this information, and shows the media dimensional stability requirements for the next 10 years including both creep and environmental effects.[1] Requirements in 2007 call for a dimensional stability of 1030 or 1000 μm/m, depending on the type of prediction scenario. By 2015, this dimensional stability requirement is projected to decrease to as low as 620 μm/m. From the data shown in Figure 10, requirements can be met in general through 2009 based on total or viscoelastic creep, dimensional stability of polyester-based PEN, and PET tapes has to be improved beyond 2009 to prevent track misregistration if total creep is considered. If the elastic response of the tape can be accounted for in the drive, viscoelastic creep response of the tapes appears to be below the dimensional stability requirements in Table III. However, it is important to note that the media dimensional stability requirements in Table III are for all effects including free thermal expansion and hygroscopic effects in addition to creep. Also, as mentioned previously, these comparisons do not account for whether or not actual tape segments widen or narrow in the pack.

In-cartridge creep specifications from PES measurements have also been presented by INSIC for current tapes with polyester substrates along with specifications for future tapes with polyester or aramid substrates. A summary of these measurements and specifications is presented in Table IV. Another TTS plot is presented in Figure 11 to facilitate a more direct comparison between the lateral creep results from creep-compliance measurements and the in-cartridge creep specifications from PES measurements in Table IV. This superposition was performed at a reference temperature of 50°C using the MP-PEN, MP-PET, and ME-Aramid data, and uses the 50 and 70°C creep-compliance data. Recall that the in-cartridge creep specifications shown in Table IV from PES measurements were determined for a 55°C, 40% RH exposure over a 10 day or 240 h time period. Although the

TABLE IV
Dimensional Stability Parameters for Tapes Using Polyester (PEN or PET) and Aramid Substrates (International Magnetic Tape Storage Roadmap, 2005, p 82, © Information Storage Industry Consortium, adapted by permission.[1])

	In-Cartridge creep[a] (μm/m)		Total stability[b] (μm/m)	
	2003–2005	2007–2015	2003–2005	2007–2015
Tapes with PEN or PET Substrates	400	300	1200	900–700
Tapes with Aramid Substrates	—	150–100	—	500–400

[a] In-Cartridge creep is measured using the position error signal (PES), and entails measuring the tape width using two servo bands. Tape width is first measured down the length of the tape at room temperature and humidity. Then, the cartridge is placed in a 55°C, 40% RH environment for 10 days, and the tape width is re-measured. In-Cartridge creep is the change in tape width.[1]

[b] Total stability includes all thermal, hygroscopic, tension, and in-cartridge creep effects.[1]

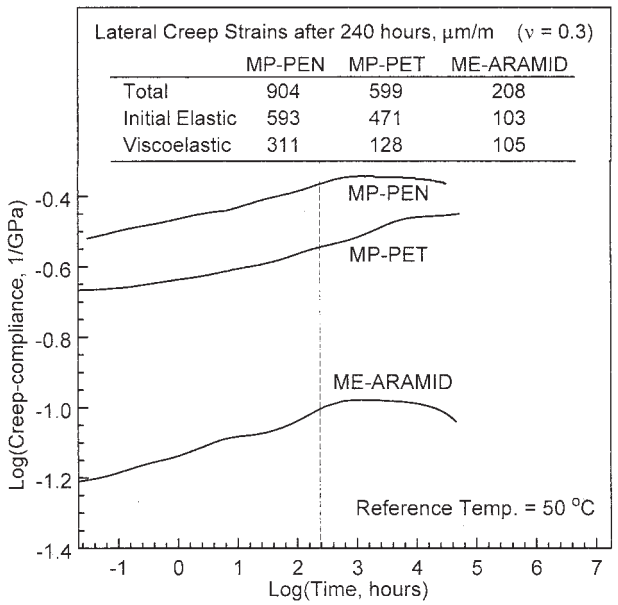

Figure 11 Creep-compliance master curves at a 50°C reference temperature using data sets fitted to the Kelvin-Voigt viscoelastic model. The master curves were generated using TTS of the curve fits for the magnetic tape materials at two temperature levels.

elevated humidity levels were not simulated during the creep-compliance measurements, the superimposed data shown in Figure 11 can be used to make a more accurate comparison with in-cartridge creep specifications from PES. After 240 h, the total lateral creep strains for MP-PEN, MP-PET, and ME-Aramid are 904, 599, and 208 μm/m, respectively. When the creep strain due to the initial elastic response is subtracted-off for each tape, the viscoelastic creep strains are 311, 128, and 105 μm/m. Since the MP-PEN and MP-PET tapes both use polyester substrates, the 400 and 300 μm/m in-cartridge creep strains shown in Table IV for the 2003–2005 and 2007–2015 time periods should be used for comparison. Using the viscoelastic creep strains from Figure 11 at 240 h, both the MP-PEN and MP-PET tapes meet the current requirements, but only MP-PET appears to meet the requirements for future tapes. Since the in-cartridge creep shown in Table IV for tapes with aramid substrates is 150–100 μm/m for the 2007–2015 time period, it appears that the ME-Aramid tape also meets the requirements for this type of tape. However, recall that the in-cartridge creep specifications from PES measurements shown in Table IV were for a 55°C, 40% RH exposure. Therefore, it should be noted that the use of a slightly higher 55°C temperature and 40% RH exposure will lead to higher creep strains for the MP-PEN, MP-PET, and ME-Aramid tapes shown in Figure 11.

CIRCUMFERENTIAL AND LATERAL CREEP STRAINS FOR MAGNETIC TAPES

Methodology

Experiments performed with the creep apparatus use a 200 mm length of tape subjected to a constant applied tensile stress. The resulting creep-compliance measurements provide fundamental information about the characteristics of the viscoelastic tape behavior. However, the constant applied tensile stress does not represent the true stress state that tapes are subjected to. Magnetic tapes are wound in a reel for storage, and they are subjected to stresses from applied tension, bending, and compression. A schematic diagram of a magnetic tape wound in a reel is shown in Figure 12. Both inner and outer wraps are subjected to tensile stresses from applied tape tension. They are also subjected to bending stresses, and as shown in Figure 12, the inner wrap is subjected to a higher bending stress than the outside wrap due to a smaller radius of curvature. Furthermore, the inner wrap is subjected to a radial compression from the rest of the tape stack. An equation for the total stress state follows:

$$\sigma_x(z) = \sigma_{\text{TENSION}} + \sigma_{\text{BENDING}} + \upsilon\sigma_{\text{RADIAL}} \tag{5}$$

where $\sigma_x(z)$ is the stress in the tape material in the x-direction as a function of distance from the hub, z (see Fig. 13); σ_{TENSION} is the stress in the tape due to applied tensile forces; σ_{BENDING} is the stress in the tape due to bending over the hub; and $\nu\sigma_{\text{RADIAL}}$ is the stress in the tape due to the Poisson's component of the radial, compressive stress, where ν is the Poisson's ratio.[4]

The tensile stress is assumed to be constant throughout the thickness of the tape, whereas the bending stress and Poisson's component of the radial stress are

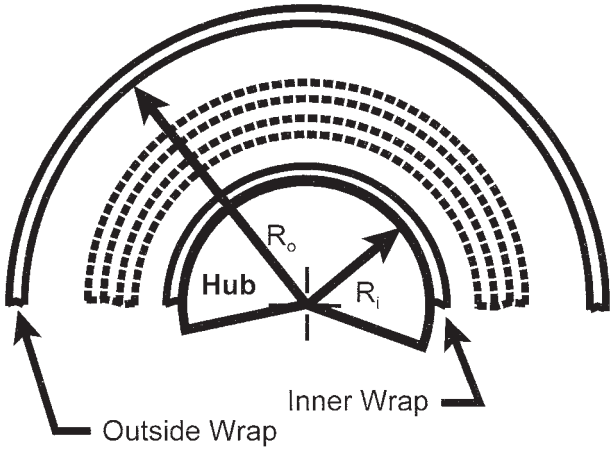

Figure 12 Schematic diagram showing tape segment wrapped around a hub.

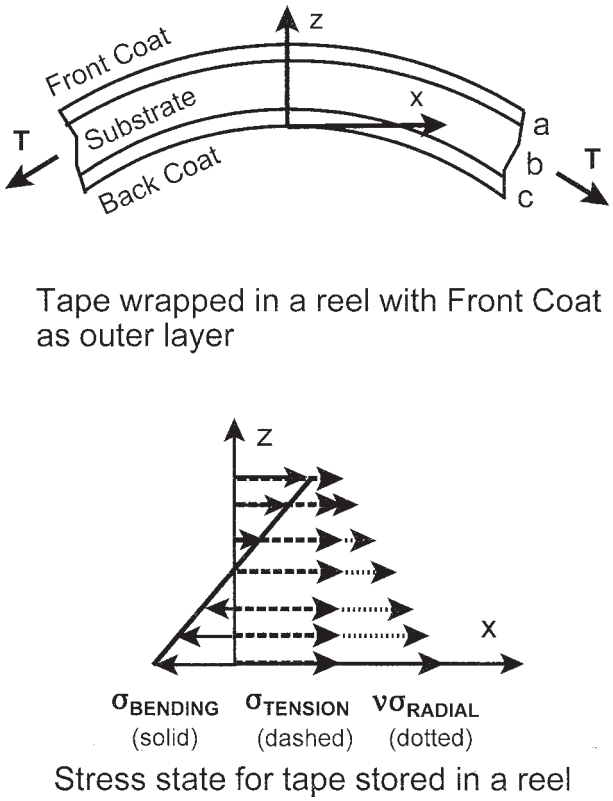

Figure 13 Stress distribution through a multiple layer magnetic tape when it is bent over a hub.

functions of z in eq. (5). Therefore, this equation is used to determine the combined stresses within each tape layer. Figure 13 provides a pictorial representation of this combined state of stress. The tape orientation is consistent with how tapes are stored in LTO, DLT, and AIT formats. The front coat is "up" and is subjected to the tensile and bending stresses. The back coat is "down," and is subjected to radial stresses in addition to the tensile and bending stresses. A more detailed review of this stress model can be found in the previous work by Weick and Bhushan.[4] Note that this is a simplified stress model that can be easily used with the experimental data to explore basic trends. More complicated models are available for calculating tape pack stresses in center-wound rolls such as those developed by Lin and Westmann[15] as well as Lee and Wickert.[16,17]

Radius values of 22 and 45 mm are used to simulate the characteristics of an LTO format reel. These radius values are particularly valid for the MP-PEN tape, which was obtained from an LTO Gen 2 cartridge. For the MP-PET and ME-Aramid tapes obtained from other formats, these radius values will still be used to foster comparisons between the three types of tapes. The tensile stress is assumed to be 7.0 MPa in eq. (5), and the radial stress is assumed to be 0 MPa at the outer wrap and 2.3 MPa at the inner wrap.[8] The 2.3 MPa radial stress assumption for the inner wrap is based on experiments performed to determine radial stresses in magnetic tapes. Bhushan[8] summarizes these experiments, which were performed at a tensile stress of 4.3 MPa, and the maximum radial stress at the hub was calculated to be 1.4 MPa. By scaling this radial stress to account for the 7.0 MPa used in this research, the radial stress was calculated to be 2.3 MPa. Previous work by Weick and Bhushan[4,5] used 1.4 MPa as the assumed radial stress. Bending stresses are at a positive maximum at the front coat, and they are at a negative maximum at the back coat. As discussed by Weick and Bhushan,[4] the inverse of the initial compliance values (D_o) can be used to estimate the elastic moduli for calculating bending stresses. Typical bending stress values for MP-PEN are 0.36 MPa at the outer wrap and 0.73 MPa at the inner wrap. For MP-PET, these values are 0.43 and 0.87 MPa at the outer and inner wraps. Values for ME-Aramid are 1.0 and 2.1 MPa at the outer and inner wraps.

Once the stress distribution through the thickness of the tape is determined using eq. (5), the strain distribution can be calculated through the tape thickness using the measured creep-compliance data for the tape, D_t (t). Equation (6) shows how this calculation is performed at a given temperature level as a function of the variables z and time to determine the circumferential strain in the tape $\varepsilon_t(z,t)$. The variable z is the through-thickness position as defined in Figure 13. Equation (7) shows how the lateral strain in the tape ε^L_t (z,t) is determined using the circumferential strain and Poisson's ratio. Note that the absolute value is used in eq. (7) to simplify graphing the information.

$$\varepsilon_t(z,t) = \sigma(z)D_t(t) \tag{6}$$

$$\varepsilon^L_t(z,t) = |-v\varepsilon_t(z,t)| \tag{7}$$

Results and discussion

Creep strain at 30 and 50°C reference temperatures for inner and outer wraps

Using the calculated stress distributions $\sigma_x(z)$ through the thickness of the tapes along with the measured creep-compliances, $D_t(t)$, and an assumed Poisson's ratio of 0.3, the circumferential and lateral strains can be calculated using eqs. (5)–(7). Graphs can be generated, which show these strains through the thickness of the tapes at creep-compliance levels corresponding to discrete times. These plots are shown in Figures 14–16 for the MP-PEN, MP-PET, and ME-Aramid tapes. The upper pair of graphs in each of these figures corresponds with a reference temperature of 30°C, and use creep-compliance information from the TTS process shown in Figure 10. The lower pair of graphs in each of these figures corresponds with a reference

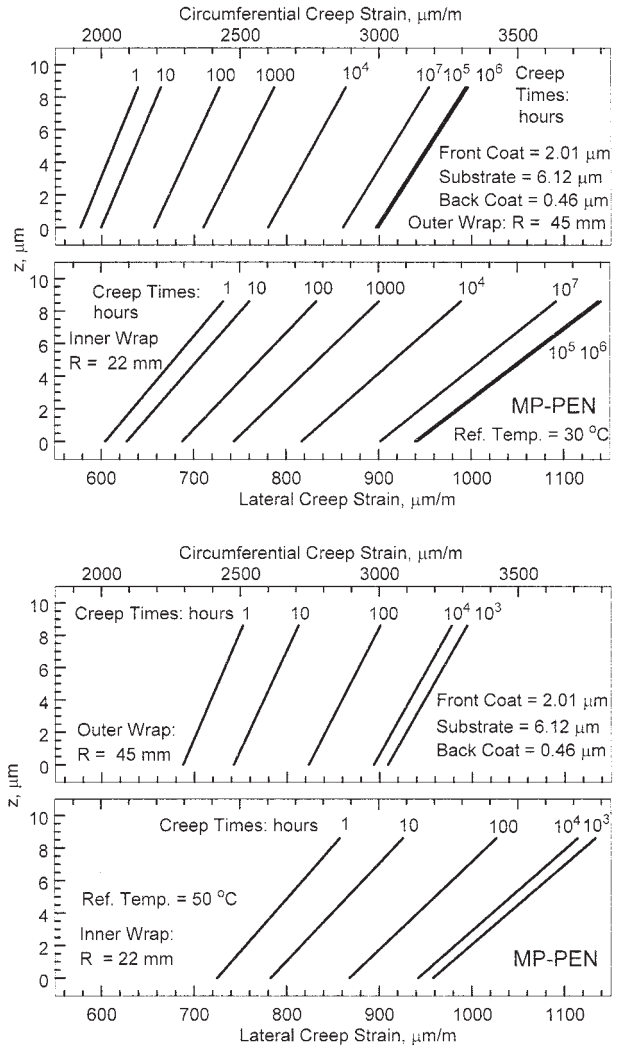

Figure 14 Circumferential and lateral strain distributions in MP-PEN tapes when they are wound in a reel. Data sets are shown for both the inner and outer wraps. The upper pair of graphs uses TTS data at a reference temperature of 30°C, and the lower pair of graphs uses data at a reference temperature of 50°C.

temperature of 50°C, and use creep-compliance information from the TTS process shown in Figure 11. Each pair of graphs shows strain information for the outer wrap in the upper panel, and the inner wrap in the lower panel. The through-thickness variable z defined in Figure 13 is plotted on the vertical axis, and lateral creep strain from eq. (7) is plotted on the lower horizontal axis. Since the Poisson's ratio of 0.3 was assumed to make the lateral creep strain calculations, it is useful to plot the circumferential creep strain on the upper horizontal axis from eq. (6). This enables readers to assume other Poisson's ratios to predict lateral creep strain. For the MP-PEN and ME-Aramid materials, as-measured thicknesses are shown for the front coat, substrate, and back coat. These thicknesses were measured by IBM for the actual tape materials used in the study, and they are slightly lower than the nominal thicknesses provided in Table I.

In general, for the three types of tapes evaluated in this study, the lateral creep strain is lower at the outer wrap than the inner wrap for a specific creep time. This is indicated by the fact that creep strain plots for the outer wrap are shifted to the left relative to creep strain plots for the inner wrap. This is due to the influence of the Poisson effect from the radial stress combined with the tension and bending of the tape. Furthermore, as expected, longer creep times lead to larger creep strains. Curves on the left-hand side of the panels represent creep strains after only 1 h, whereas curves on the right-hand side of the panels represent longer creep times of 10^5 to 10^7 h for a reference temperature of 30°C, or 10^4 h for a reference temper-

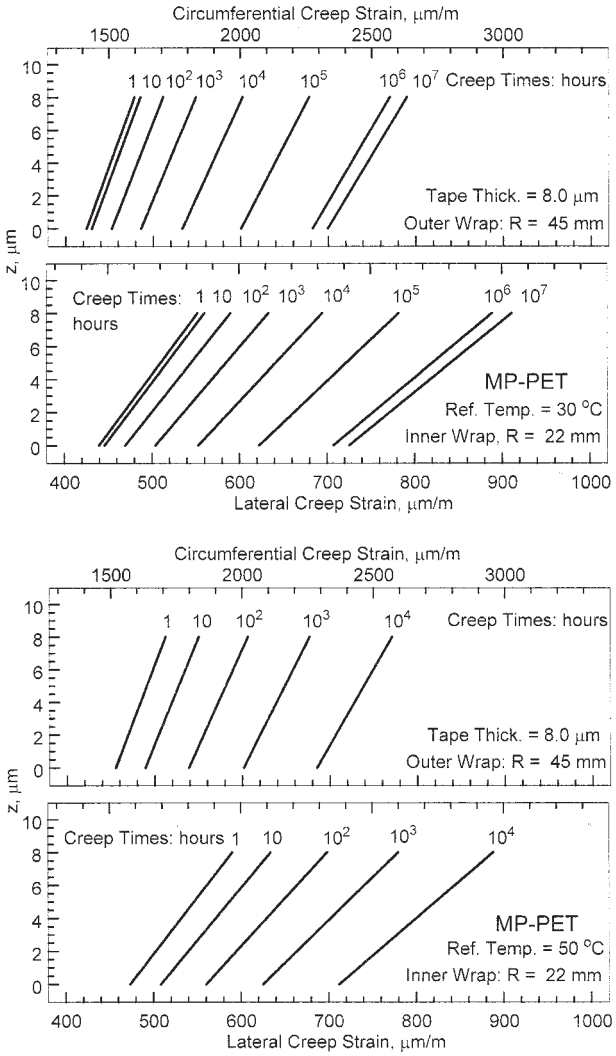

Figure 15 Circumferential and lateral strain distributions in MP-PET tapes when they are wound in a reel. Data sets are shown for both the inner and outer wraps. The upper pair of graphs uses TTS data at a reference temperature of 30°C, and the lower pair of graphs uses data at a reference temperature of 50°C.

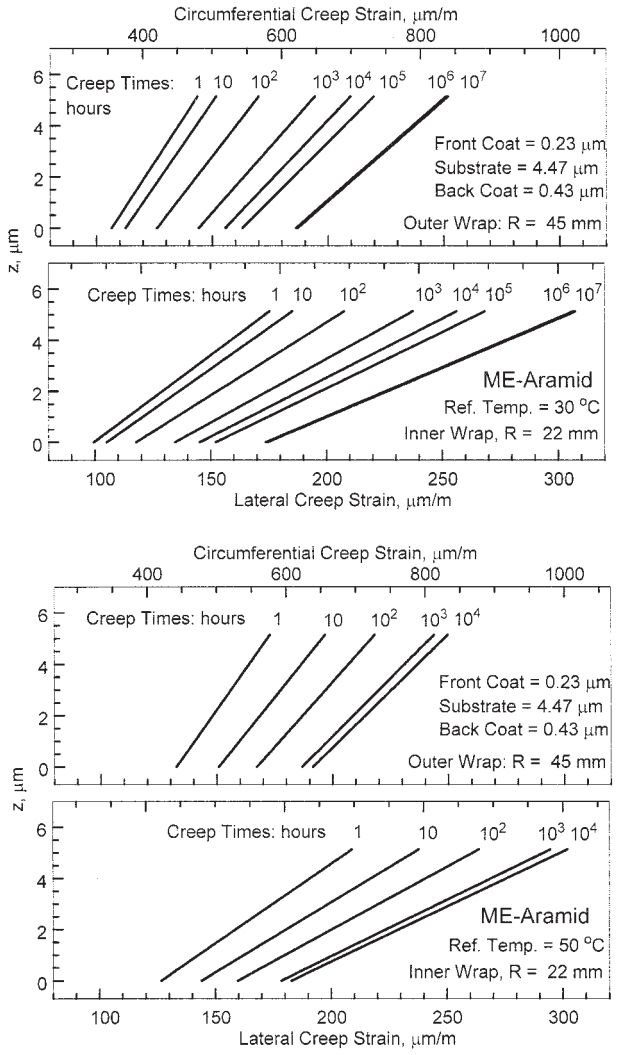

Figure 16 Circumferential and lateral strain distributions in ME-Aramid tapes when they are wound in a reel. Data sets are shown for both the inner and outer wraps. The upper pair of graphs uses TTS data at a reference temperature of 30°C, and the lower pair of graphs uses data at a reference temperature of 50°C.

ature of 50°C. In addition, the slopes of the lines for the inner wrap tend to be greater than the slopes of the lines for the outer wrap. This indicates that there is a greater change in creep strain through the thickness of a tape segment at the inner wrap when compared with a tape segment at the outer wrap. Furthermore, the creep strain at the front coat of the tape is predicted to be larger than the creep strain at the back coat of the tape, and this difference is greater for the inner wrap versus the outer wrap as indicated by the slopes of the lines.

For the MP-PEN tape at a reference temperature of 30°C, the creep strains shown in Figure 14 after 10^7 h appear to be lower than the creep strains after 10^5 or 10^6 h. This is due to the decrease in creep-compliance after 10^5 h observed in the superimposed data shown in Figure 10 for a reference temperature of 30°C. This is also observed in the MP-PEN creep strains for a 50°C reference temperature; the creep strain after 10^4 h is lower than the creep strain after 10^3 h. For the reference temperature of 30°C, the lateral creep strain in the outer wrap approaches a maximum of 1000 μm/m after a creep time of 10^6 h. In comparison, the maximum creep strain in the inner wrap is higher and is 1140 μm/m after 10^6 h. If the 559 μm/m initial elastic response from Figure 10 is subtracted-off, then the viscoelastic lateral creep strains can be calculated to be 441 and 581 μm/m, respectively. These values are below the dimensional stability parameters shown in Table III for future magnetic tapes. However, as mentioned previously, the parameters in Table III include all environmental effects in addition to creep.

To facilitate comparisons with tape substrate in-cartridge creep specifications listed in Table IV, the creep strains at 50°C in the lower pair of graphs can be used. Recall that the in-cartridge creep specifications in Table IV are lateral specifications obtained using the PES from the tape after the cartridge is exposed to a 55°C, 40% RH environment for 10 days (240 h). Actual in-cartridge creep measurements for 2003 are shown for tapes with polyester substrates, and specifications for future tapes with polyester or aramid substrates are shown for the 2007–2015 time frame. At 240 h, the lower pair of graphs in Figure 14 shows that the lateral creep strain will exceed 900 μm/m at the top of the outer wrap, and exceed 1020 μm/m at the top of the inner wrap. This information was obtained by reading the lateral creep strain at the peaks of the 100 h creep time lines. By subtracting-off the 593 μm/m initial elastic response shown in Figure 11, the viscoelastic lateral creep strains can be calculated to be 307 and 427 μm/m at the outer and inner wraps. These values exceed the 300 μm/m specification shown in Table IV for future tapes with polyester substrates. Note that the simplified stress model used to calculate the stresses at the outer and inner wraps could lead to overestimates of creep strain.

Creep strain results for MP-PET shown in Figure 15 tend to be lower than those measured for MP-PEN, which is consistent with the lower creep-compliances shown in the superimposed plots of Figures 10 and 11. Lateral creep strains at a reference temperature of 30°C shown in the upper pair of figures approach 800 μm/m in the outer wrap, and 920 μm/m in the inner wrap for a creep time of 10^7 h. When the initial elastic response of 438 μm/m is subtracted-off, the viscoelastic lateral creep strains can be calculated to be 362 and 482 μm/m, respectively. These lateral creep strains are lower than those specified in Table III for future magnetic tapes, although once again it needs to be stated that all environmental influences are included in the parameters shown in Table III. At a reference temperature of 50°C, maximum lateral creep strains after

100 h are 680 μm/m in the outer wrap and 700 μm/m in the inner wrap, with corresponding viscoelastic lateral strains of 205 and 229 μm/m. These values are below the in-cartridge creep parameters specified in Table IV. It should be noted that the lower creep-compliance for the tensilized PET used for the MP-PET tape could be the reason why the lateral creep strain for the MP-PET tape is lower when compared with the MP-PEN tape.

From Figure 16, ME-Aramid tape shows the lowest overall creep strain when stored in a reel, which corresponds with the lower overall creep-compliance shown in Figures 10 and 11. At a reference temperature of 30°C, lateral creep strains approach 250 μm/m in the outer wrap and are greater than 300 μm/m in the inner wrap after 10^7 h. By subtracting-off the initial elastic response of 113 μm/m, the viscoelastic lateral strains can be calculated to be 137 and 187 μm/m at the outer and inner wraps. This shows that the ME-Aramid tape could meet dimensional stability requirements shown in Table III out to 2015 if additional environmental contributions are not substantial. When the lower pair of graphs in Figure 16 at a reference temperature of 50°C is used to make comparisons with the in-cartridge creep specifications from PES measurements shown in Table IV, the ME-Aramid tape appears to show lateral creep characteristics that are higher than what is targeted for future tapes with aramid substrates. At 50°C after 100 h, the lateral creep strain at the outer wrap of the ME-Aramid tape approaches 220 μm/m, and is approximately 240 μm/m at the inner wrap. This corresponds with lateral viscoelastic strains of 117 and 137 μm/m for the outer and inner wraps using the initial elastic response of 103 μm/m. These values are below the 150 μm/m in-cartridge creep specification shown in Table IV. This shows once again that current aramid-based tapes can meet future requirements, although the high cost of the aramid substrate could make this unfeasible in certain tape applications.

Creep strain predictions for thinner, lower compliance magnetic tape materials

Future magnetic tapes are projected to have thinner front coats, which consist of magnetic and nonmagnetic layers. Reduction in substrate thickness is also projected for the future, and thinner layers will enable more tape to be stored in a reel. Reductions in compliance are also predicted for the constitutive layers of the tape, and the combined reduction of thickness and compliance is of interest to tape manufacturers.

Using the methodology discussed in the previous section for predicting the creep strain on a tape through the thickness of the tape, it is possible to simulate how the creep strain would change under the following scenarios: (i) front coat thickness reduced by 1/3, (ii) front coat and substrate thickness reduced by 1/3, (iii) tape compliance reduced by 1/3, and (iv) compliance and thickness of the tape reduced by 1/3. Creep strain calculations were performed using these scenarios, and results are shown in Figures 17–19 for MP-PEN, MP-PET, and ME-Aramid tapes, respectively. In each of the scenarios, the creep strains were calculated using creep-compliance information shown in Figure 10 at a reference temperature of 30°C. Creep strains calculated for the actual tape thickness and compliance are shown as dashed lines in Figures 17–19, and these creep strains are identical to the ones presented in Figures 14–16 for a 30°C reference temperature. This enables direct comparisons to be made between the simulated situation represented by the solid lines, and the base-case situation for the actual tape represented by the dashed lines. Note that the dashed lines represent as-measured layer thicknesses for the MP-PEN and ME-Aramid tapes in Figures 17 and 19, whereas nominal layer thicknesses are used for MP-PET in Figure 18.

Reduction of the front coat thickness by 1/3 appears to lead to a slight increase in creep strain, and a 1/3 reduction of the front coat and substrate thickness appears to lead to a greater increase in creep strain. This was observed for all three tape materials, and is shown in the top two graphs in Figures 17–19 for the inner and outer wraps. The solid lines that represent the simulated situation are shifted to the left of the dashed lines that represent the creep strain for the actual tape. For ME-Aramid, the reduction in front coat thickness causes a minimal change in creep strain, and the solid and dashed lines appear to be superimposed on one another.

When tape compliance is reduced by 1/3, the creep strains are significantly reduced and shift to the left. For longer creep times of 10^5 to 10^7 h, this 1/3 compliance reduction can lead to decreases in lateral creep strain of 350 μm/m at the inner wrap for MP-PEN, with decreases of 270 μm/m for MP-PET, and decreases of 80 μm/m for ME-Aramid at the inner wrap. Decreases in lateral creep strain at the outer wraps are somewhat less with decreases of 320, 250, and 70 μm/m observed for MP-PEN, MP-PET, and ME-Aramid at longer creep times of 10^5 to 10^7 h. For shorter creep times of 1 h, a 1/3 tape compliance reduction leads to smaller decreases in lateral creep strain. At the inner wrap, lateral creep strain decreases of 220, 170, and 50 μm/m are shown for the three respective tape materials at a creep time of 1 h, and these decreases are even less at the outer wrap.

The reduction of compliance and thickness by 1/3 also leads to a decrease in creep strain, but this decrease is not as significant as that observed for compliance reduction alone. Recall that a thickness reduction alone causes a slight increase in creep strain, and this partially offsets the decrease in creep strain ob-

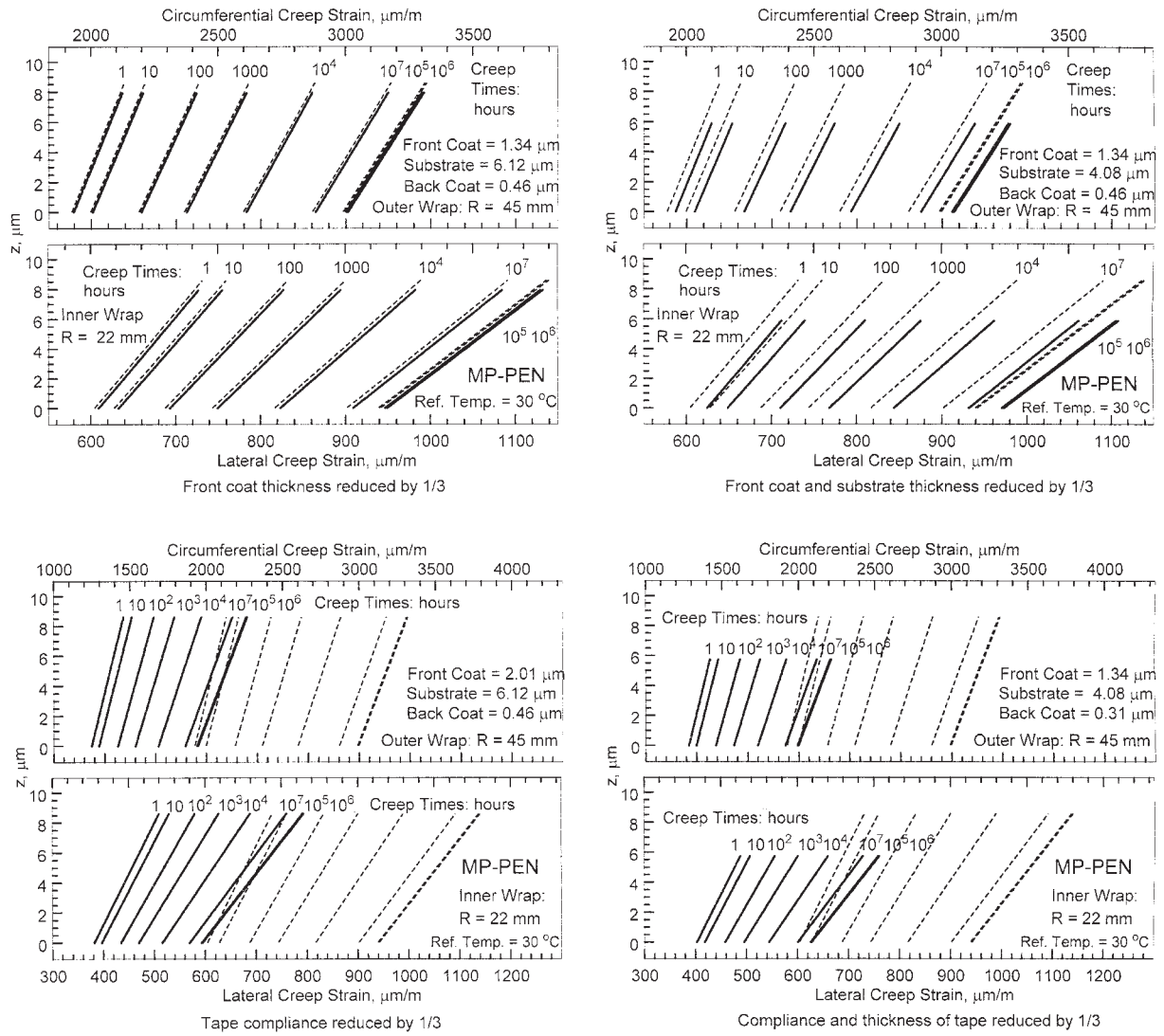

Figure 17 Predicted strain distributions in an MP-PEN tape of varying construction/design when it is wound in a reel. Data sets are shown for both the inner and outer wraps at a reference temperature of 30°C. The hub radius is assumed to be 22 mm, and the outer radius of the reel is assumed to be 45 mm.

served when compliance is reduced. Lateral creep strain decreases of 380, 300, and 100 μm/m are shown for the MP-PEN, MP-PET, and ME-Aramid materials at longer creep times of 10^5 to 10^7 at the inner wrap. Once again, these decreases are less significant at the outer wrap, and shorter creep times of 1 h lead to smaller decreases in creep strain.

COMPLIANCE AND STRESSES FOR CONSTITUTIVE MP-PEN TAPE LAYERS

Methodology

Additional experiments were performed using specially-prepared MP-PEN samples to determine the properties of the front coat (magnetic and nonmagnetic layer), substrate, and back coat. The procedure calls for the magnetic tape to be modeled as a multiple layer polymer composite laminate as shown in Figure 20. It utilizes a rule of mixtures method to predict the creep-compliance of a whole tape if the creep-compliances of each layer are known. Jones[18] provides an excellent review of the rule of mixtures method, and Weick and Bhushan[4,5] demonstrated the applicability of this method for predicting the behavior of magnetic tapes. They also provide an extensive discussion of this methodology,[4] which will be summarized herein.

Using the equation shown below, the creep-compliance of the front coat can be determined if data are available from creep-compliance experiments performed using a front coat + substrate material and the substrate only. See Figure 20 for nomenclature, and Weick and Bhushan[4,5] discuss the technique used to prepare the dual-layer samples.

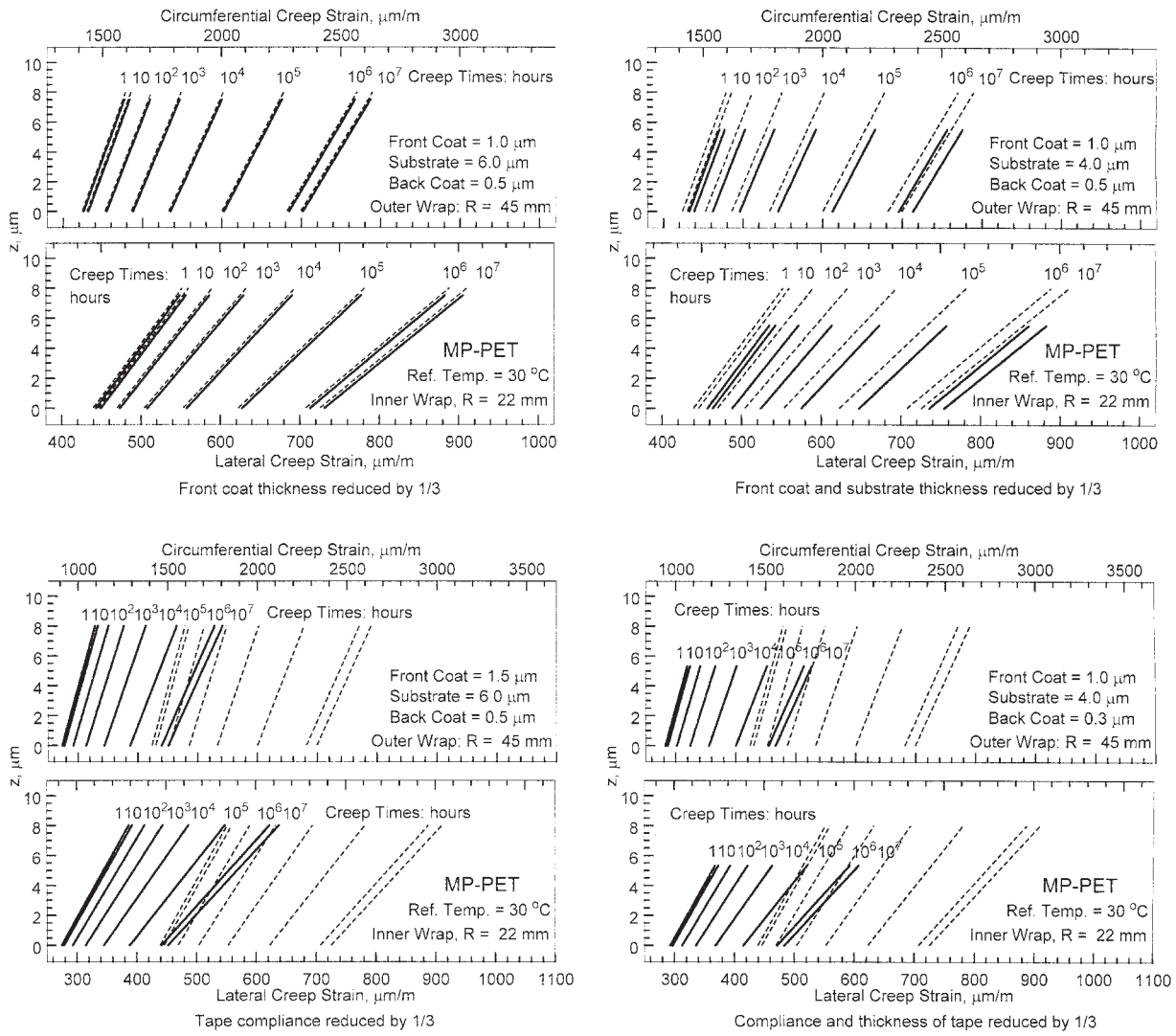

Figure 18 Predicted strain distributions in an MP-PET tape of varying construction/design when it is wound in a reel. Data sets are shown for both the inner and outer wraps at a reference temperature of 30°C. The hub radius is assumed to be 22 mm, and the outer radius of the reel is assumed to be 45 mm.

$$D_a(t) = \left[\left(\frac{a+b}{a}\right)\left(\frac{1}{D_{ab}(t)}\right) - \left(\frac{b}{a}\right)\left(\frac{1}{D_b(t)}\right)\right]^{-1} \tag{8a}$$

Similarly, the creep-compliance of the back coat can be determined if data are available from creep-compliance experiments performed using a substrate + back coat material and the substrate only.

$$D_c(t) = \left[\left(\frac{b+c}{c}\right)\left(\frac{1}{D_{bc}(t)}\right) - \left(\frac{b}{c}\right)\left(\frac{1}{D_b(t)}\right)\right]^{-1} \tag{8b}$$

Once the creep-compliances of the front coat and back coat have been determined using eqs. (8a) and (8b), the creep-compliance for a complete tape can be predicted using eq. (8c).

$$D_t(t) = \left[\frac{1}{h}\left(\frac{a}{D_a(t)} + \frac{b}{D_b(t)} + \frac{c}{D_c(t)}\right)\right]^{-1} \tag{8c}$$

Data sets determined using eq. (8c) for a complete tape use creep-compliance data for the front coat, substrate, and back coat from three separate experiments. To verify this technique, the data sets determined using eq. (8c) can be compared with actual measured data sets for a magnetic tape.

Time–temperature superposition for the MP-PEN constitutive tape materials, and determination of the front coat and back coat compliances

Raw data acquired at 30, 50, and 70°C for the MP-PEN tape, substrate, front coat + substrate, and substrate + back coat were fitted to the Kelvin-Voigt model, and the fitted data sets are shown in Figure 21. These data

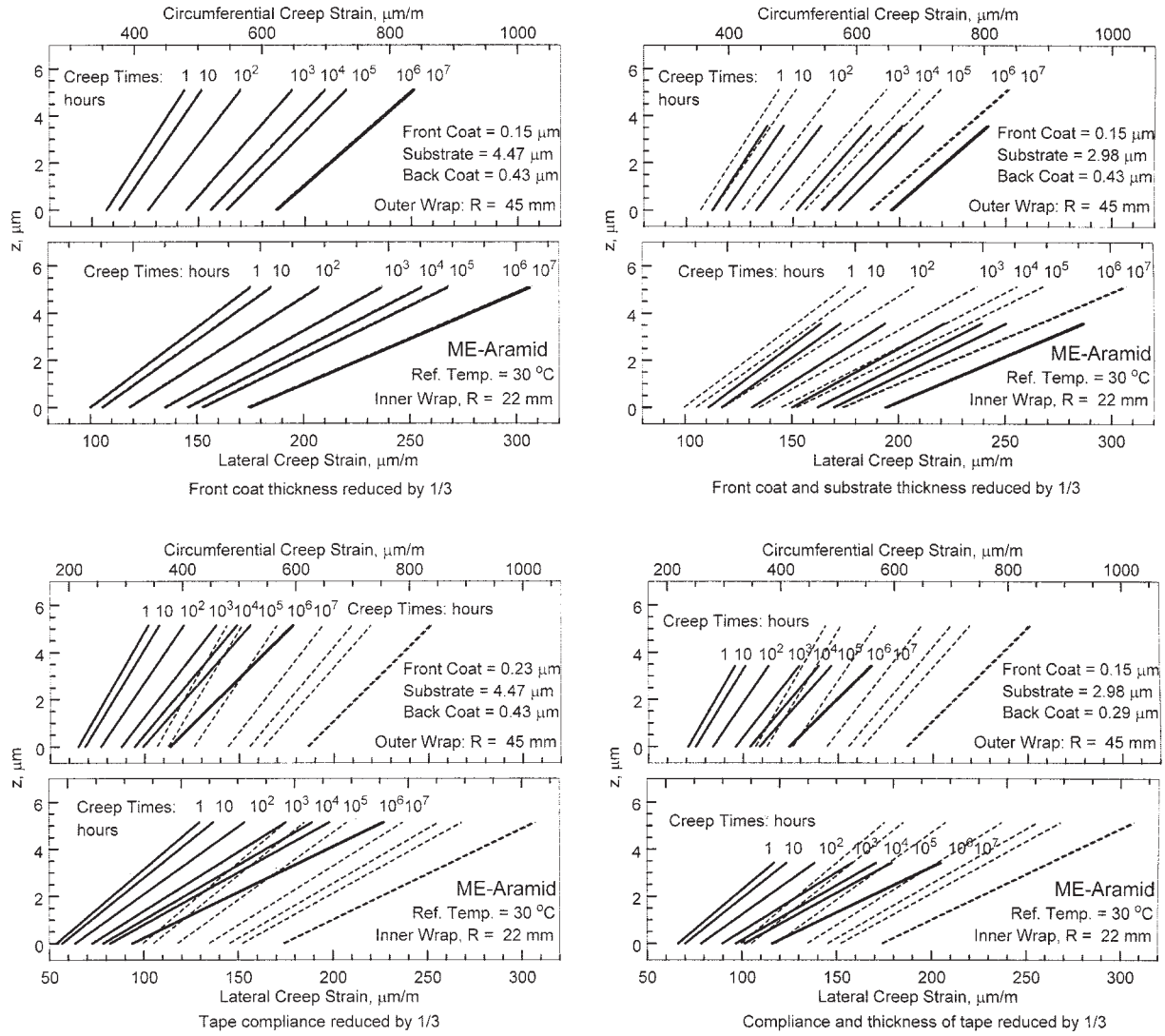

Figure 19 Predicted strain distributions in an ME-Aramid tape of varying construction/design when it is wound in a reel. Data sets are shown for both the inner and outer wraps at a reference temperature of 30°C. The hub radius is assumed to be 22 mm, and the outer radius of the reel is assumed to be 45 mm.

sets were then used in the TTS process to develop the master curves shown in Figure 22 for a reference temperature of 30°C. Equations (8a) and (8b) were then used to calculate the creep-compliances for the front coat and back coat over extended time periods, and these plots are shown in Figure 23. Finally, eq. (8c) was used to calculate a creep-compliance for the magnetic tape based on the measured compliance for the substrate and compliances for the front coat and back coat that were determined using eqs. (8a) and (8c)from the dual-layer experiments.

From Figures 21 and 22, the creep-compliance for the front coat + substrate is higher than the compliance measured for the tape and substrate. Therefore, it would seem that the front coat plays a significant role in determining the creep behavior of the tape. As shown in Figure 23, the front coat also appears to have a higher creep-compliance and increasing trend to its creep behavior when eq. (8a) is used to extract the compliance of the front coat using the measured substrate and front coat + substrate creep-compliances. Weick and Bhushan[5] have attributed this behavior to the elastomeric nature of the binder used in the front coat for the MP coating, which is likely to be very susceptible to creep. The front coat is also considered to be nonisotropic, which could contribute to lateral creep characteristics that are different from the longitudinal creep, although experiments presented herein were not designed to address this issue. In comparison, the compliance of the PEN substrate is less than the tape or front coat + substrate, and this could be attributed to stronger intermolecular bonds in the polyester substrate material as well as inhibition of intermolecular movements and side chain movements. These intermolecular motions are what cause creep in polymer materials, and the PEN substrate is

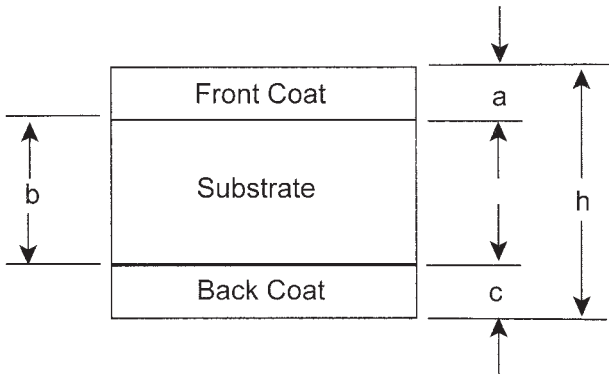

Subscripts

a, b, c — front coat, substrate, back coat

t — tape

ab — combined front coat and substrate

bc — combined substrate and back coat

Figure 20 Nomenclature used to describe tape layers.

likely to be less susceptible to these types of motions than the elastomeric binder used for the magnetic coating.

Differences in creep-compliance could not be easily determined for the back coat + substrate dual-layer material. From Figure 22, the creep-compliance of the back coat + substrate follows the creep-compliance of the substrate very closely. The nominal 0.5-μm-thick back coat is significantly thinner than the substrate, and its contribution to the compliance of the combined substrate + back coat sample could be minimal. When the back coat compliance is extracted-out and shown in Figure 23, the small difference between the substrate and back coat + substrate creep-compliance leads to variations in the back coat creep-compliance. The actual back coat compliance calculated using eq. (8b) is shown by the solid line in Figure 23, and the dashed line shows the increasing trend to the data. This increasing trend to the back coat compliance data initially follows the trend to the substrate data, but continues to increase above that measured for the substrate.

To determine the validity of the front coat and back coat compliances calculated using eqs. (8a) and (8b), the creep-compliance for the tape is calculated using eq. (8c). The calculated creep-compliance for the tape based on front coat, substrate, and back coat compliances is plotted in Figure 24 and compared with the measured creep-compliance for the MP-PEN tape. During the initial 100 h, the creep-compliance for the calculated and measured tapes shows a close correspondence. After approximately 100 h, the deviation between the calculated and measured compliances increases, but this deviation does not change significantly until 10^5 h. At that point, the measured creep-

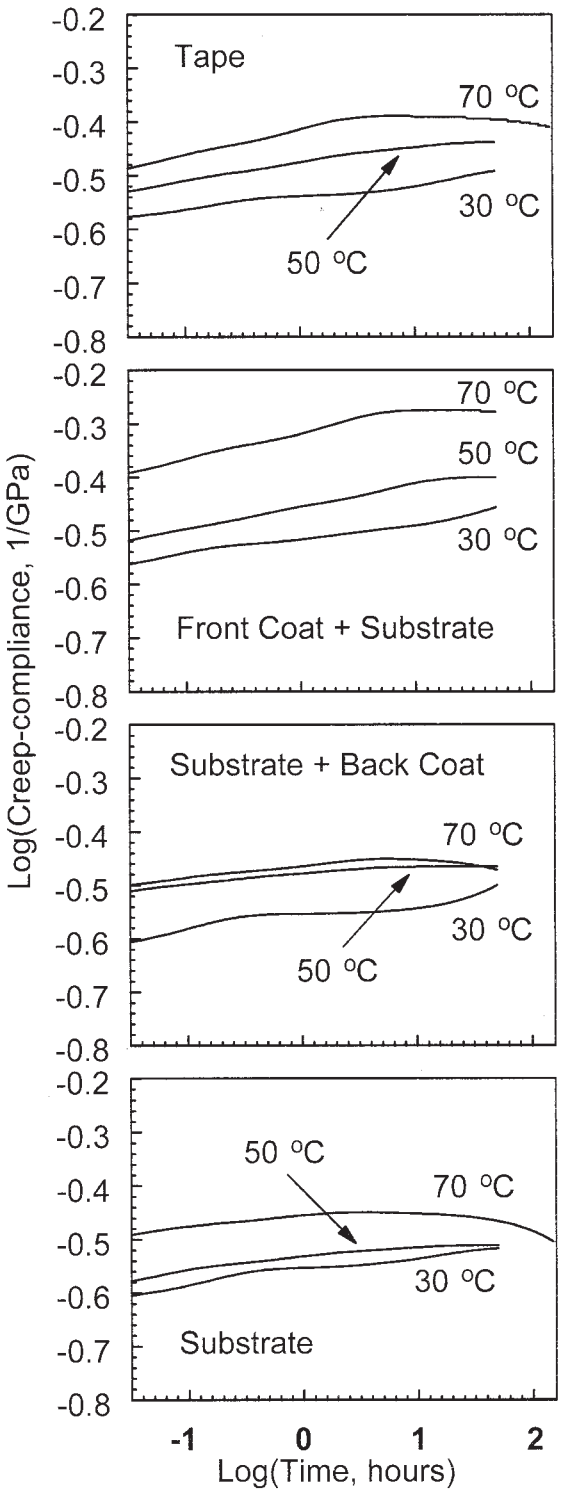

Figure 21 Creep-compliance curves for MP-PEN tape, substrate, and dual-layer front coat + substrate and back coat + substrate samples. Curve fits are shown after fitting the data sets to a Kelvin-Voigt model.

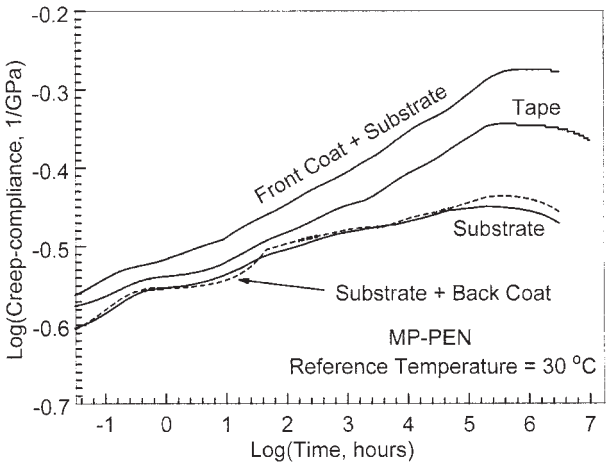

Figure 22 Creep-compliance master curves for MP-PEN tape, substrate, and dual-layer samples at a 30°C reference temperature. The master curves were generated using TTS of the curve fits for data sets at three temperature levels.

compliance appears to undergo a more pronounced decrease than the calculated compliance. The deviation between the calculated and measured compliances could be due to the difficulty in extracting the back coat compliance from the back coat + substrate measurements. Previous work by Weick and Bhushan[5] with PET-based tapes have shown that the back coat compliance is indeed lower than the substrate compliance because of the typical use of nitrocellulose-based polymers for the back coat material. A lower back coat compliance would bring the calculated creep-compliance for the MP-PEN tape closer to the measured creep-compliance.

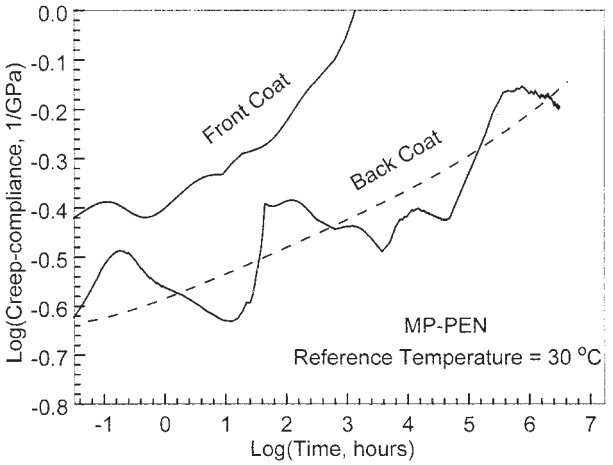

Figure 23 Creep-compliance master curves at a 30°C reference temperature for the front coat and back coat of an MP-PEN tape. These curves were generated using a rule-of-mixtures model and experimental results for the substrate and dual-layer front coat + substrate and back coat + substrate samples.

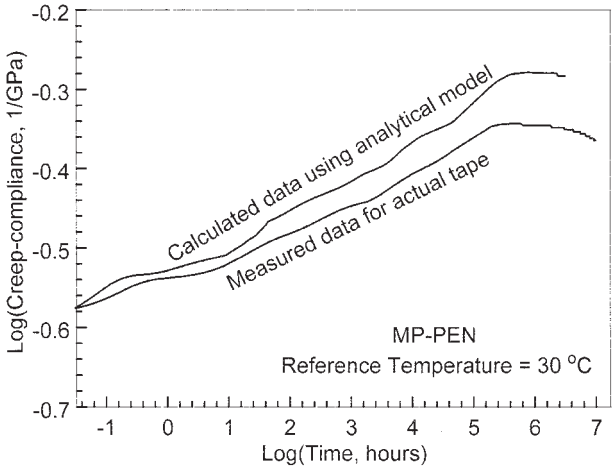

Figure 24 Comparison of calculated and measured creep-compliances for an MP-PEN tape. The calculated data were determined using front coat and back coat data sets generated using the rule-of-mixtures model together with experimental results for the substrate. Creep-compliance experiments were performed for the complete MP-PEN tape to determine the experimental data.

Stresses in the constitutive layers of MP-PEN tape

Using the reel model shown in Figures 12 and 13 together with the compliances for the front coat, back coat, and substrate, stresses can be calculated for the constitutive layers of the MP-PEN tape. Equations (9a)–(9c) show how these stresses can be calculated for each layer using the strain calculated for the tape and the compliances of the layers.

$$\sigma_a(z,t) = \varepsilon_t(z,t)/D_a(t) \tag{9a}$$

$$\sigma_b(z,t) = \varepsilon_t(z,t)/D_b(t) \tag{9b}$$

$$\sigma_c(z,t) = \varepsilon_t(z,t)/D_c(t) \tag{9c}$$

The subscript a, b, c, and t denote properties for the front coat, substrate, back coat, and tape as defined in Figure 20. Note that the stresses and strains are a function of time as well as the through-thickness variable z defined in Figure 13. The compliances are constant for each layer, but are also functions of time.

Using eqs. (9a)–(9c), the stresses through the thickness of the MP-PEN tape are plotted in Figure 25 for the inner and outer wraps. As-measured thicknesses are used for Figure 25, which were provided by IBM for the actual MP-PEN tape used in the study. Note that the stress, $\sigma_x(z)$, is also plotted for the complete tape as calculated using eq. (5). This stress is shown as a dashed line in Figure 25. The solid lines show the stresses in the tape layers at discrete creep times. For the front coat, longer creep

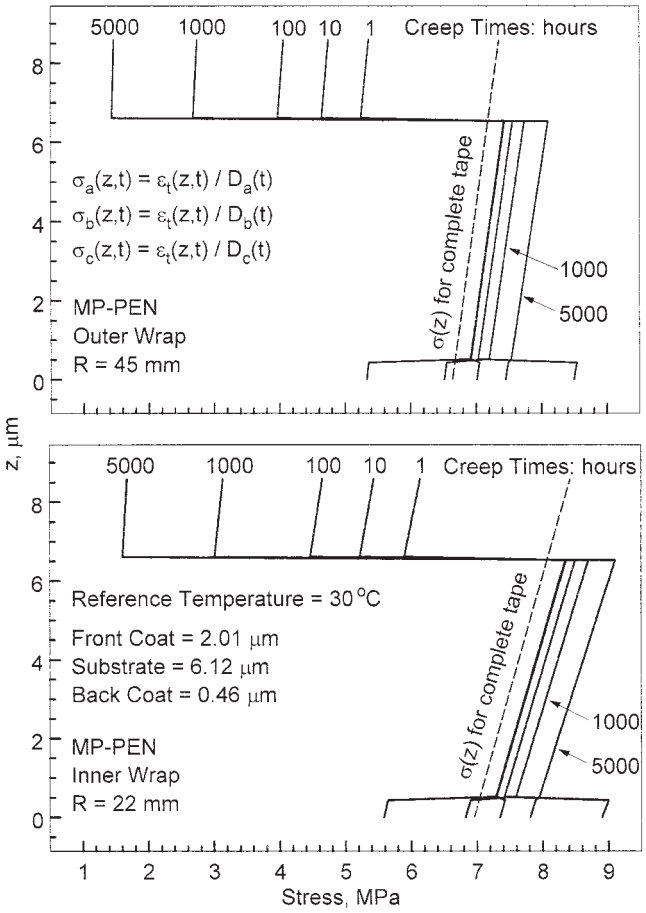

Figure 25 Stress distributions for a complete MP-PEN tape (dashed line), and stress distribution calculations based on creep-compliances (D_a, D_b, D_c) determined for the tape layers using the rule-of-mixtures model.

times lead to lower stresses because of the increase in compliance for the front coat as a function of time. In comparison, creep times beyond 1000 h cause a decrease in compliance for the substrate. Stresses for the back coat vary significantly, which is consistent with the variation in back coat compliance shown in Figure 23. Stresses in the outer wrap also tend to be lower than stresses in the inner wrap because of the lower creep strains calculated for the outer wrap. Furthermore, the change in stress through the thickness of the tape appears to be greater for the inner versus the outer wrap, which is again consistent with the strain behavior. Figure 25 shows how creep of the tape when it is stored in a reel can lead to a reduction in the stress on the tape. Furthermore, it shows how changes in stress distribution through the tape can also be influenced by creep. This could lead to loose wraps and inconsistent stress profiles that could manifest itself as lost information when the head tries to read information from the tape.

ADDITIONAL EXPERIMENTS: CREEP RECOVERY AND SHRINKAGE

Creep recovery

Additional information can be extracted from the creep experiments performed using the magnetic tape materials. A 50 h creep experiment is normally followed by a 50 h recovery period. An example of a complete creep and recovery experiment is shown in Figure 26 for MP-PEN and MP-PET on a linear scale rather than the log scales used for previous figures. The constant 7.0 MPa stress is applied to the magnetic tapes during the first 50 h, and this causes the tapes to creep during that time period. After the 50 h, the stress is removed and the tapes are allowed to recover. Note that MP-PET does not appear to recover completely, whereas MP-PEN does recover completely in less than 50 h. Previous work by Weick and Bhushan[3] showed that PEN substrates do have shorter recover time periods than PET. Furthermore, PET has been shown to not recover completely, possibly due to plastic deformation.[3,8,9]

In Figure 27, creep recovery characteristics for the MP-PET, MP-PEN, and ME-Aramid tapes are shown on one plot along with the creep recovery for the PEN substrate. Recall that creep behavior for the PEN substrate was measured for the rule of mixtures model, and is shown in Figure 21. Repeat experiments are depicted to show the repeatability of the recovery experiments. Figure 27 once again shows that creep recovery for the MP-PEN tape descends to zero or near zero levels, whereas the creep recovery for the MP-PET tape does not recover completely even after 100 h. The creep recovery for the PEN substrate appears to occur over a shorter time period than the recovery for the MP-PEN tape as a whole, which suggests that the presence of the front coat and/or back coat materials could play a role in inhibiting

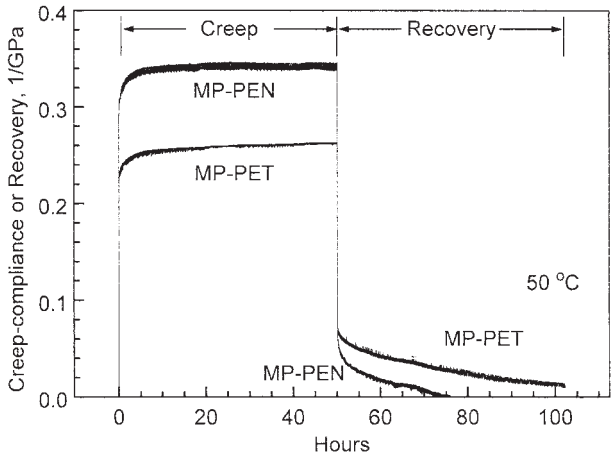

Figure 26 Examples of 100 h creep-compliance and recovery experiments for MP-PEN and MP-PET.

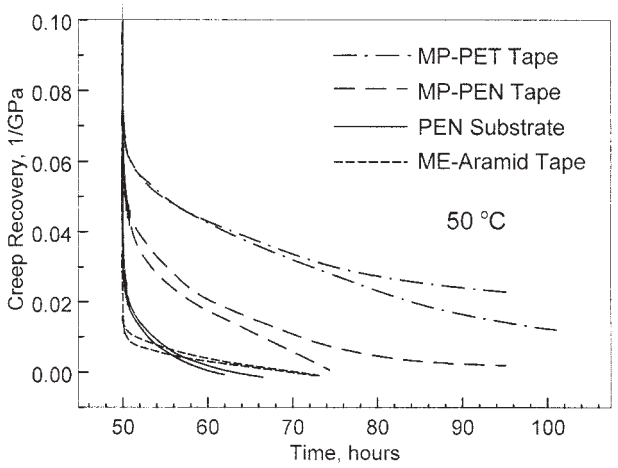

Figure 27 Creep recovery data for MP-PEN, MP-PET, and ME-Aramid tapes along with a PEN substrate. Repeat experiments are shown for each tape or substrate.

creep recovery. Finally, Figure 27 also shows that the ME-Aramid tape recovers over a relatively short time period.

Shrinkage

Prior to starting a creep experiment by dropping the weights remotely as shown in Figure 1, the test chamber is allowed to warm-up. This warm-up period is normally 10 h, and allows the test chamber to come up to the preset temperature. During this time period, the tapes are subjected to a minimal 0.5 MPa stress to keep them between the grips of the test apparatus. As the chamber warms-up, there is some minimal thermal expansion of the test apparatus that stops once the preset temperature is reached. Because of the structure of the apparatus and mounts used for the LVDT position sensors, as the apparatus expands, there is a rapid decrease in the signals from the LVDT's. Once the preset temperature is reached, the apparatus stops expanding, but the tape samples continue to shrink because of the mechanisms described by Weick and Bhushan.[3,19] It should also be noted that the hygroscopic characteristics of the tapes could also contribute to the shrinkage characteristics.

Figure 28 depicts the shrinkage of the magnetic tape materials used in this study. Temperature is shown as a dotted line, and is read from the right-hand axis. Note that the preset temperature of 49.8°C is reached after 2 h, but the samples continue to shrink beyond this time period. Consistent with past work by Weick and Bhushan,[19] the MP-PEN tape and PEN substrate shrink the most when compared with MP-PET and ME-Aramid. The ME-Aramid shrinks the least, and appears to reach a plateau.

Shrinkage of the magnetic tapes can be directly attributed to the polymeric structure of the magnetic tape materials. It is a nonrecoverable deformation process that can be attributed to relaxation of partially-oriented molecules in the amorphous regions of the polymer, and could result in removal of the residual stresses formed during processing of the tape.[3,9] The crystalline regions do not contribute to shrinkage behavior. Below the glass transition temperature for its PET substrate, MP-PET tape would not be expected to undergo a substantial amount of shrinkage, which appears to be the case when compared with MP-PEN. The same should be true for MP-PEN and it's PEN substrate; however, it does exhibit comparatively substantial shrinkage behavior. Weick and Bhushan[3] also observed this for PEN substrates, and attributed this behavior to steric hindrance caused by the naphthalene ring in PEN. This could cause some of the PEN macromolecules to be frozen into a partially-oriented amorphous phase. When the polymer is heated, energy transfer to these partially oriented molecules could allow them to reorient to shorter lengths causing shrinkage.[3] Last, the rigid rod-like structures for the ME-Aramid substrate exhibit a high degree of orientation, and shrinkage should be minimized. The shrinkage that does occur in the ME-Aramid tape could be attributed to the sulfone groups in the aramid substrate back bone that could inhibit crystallization and lead to shrinkage from the rearrangement of partially oriented molecules.[3]

SUMMARY AND CONCLUSIONS

Creep-compliance experiments were presented for three representative magnetic tape materials: MP-PEN, MP-PET, and ME-Aramid. Experiments were performed at 30, 50, and 70°C, and TTS was used to predict creep behavior at 30 and 50°C reference temperatures. A Kelvin-Voigt viscoelastic model was also used to obtain curve fits for the data, and continuous data sets were constructed using the TTS process. In

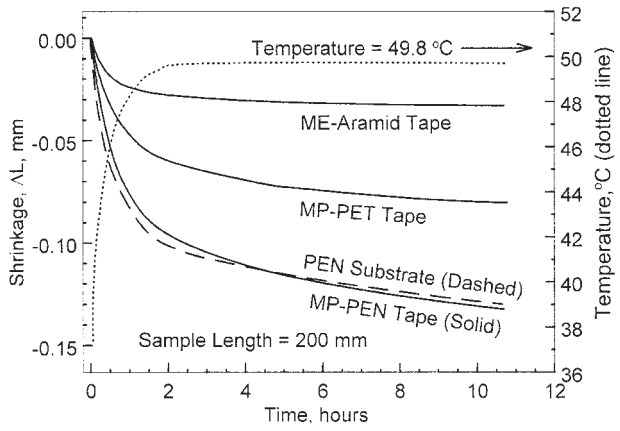

Figure 28 Shrinkage data for MP-PEN, MP-PET, and ME-Aramid tapes along with a PEN substrate.

general, creep-compliances for the polyester-based tapes (MP-PEN and MP-PET) were higher than what was measured for ME-Aramid. This was attributed to the lower compliance aramid substrate used for the ME-Aramid tape. The creep-compliance for the MP-PEN tape also appeared to be higher than what was measured for the MP-PET tape. However, because of possible molecular movements after long time periods, the rate of creep-compliance for the MP-PEN tape appeared to decrease more at longer creep times for a 30°C reference temperature when compared with MP-PET.

Comparisons were made with available PES specifications for dimensional stability requirements and in-cartridge creep specifications from PES measurements for tapes with polyester or aramid substrates. From the creep-compliance measurements presented herein along with an assumed Poisson's ratio of 0.3, dimensional stability requirements for future magnetic tapes shown in Table III can be met through 2009 if total creep is considered including elastic and viscoelastic effects. Dimensional stability must be improved to prevent track misregistration beyond that time period if total creep is considered, but viscoelastic lateral creep strains are below the stability requirements for 2015. However, media dimensional stability requirements in Table III are for all effects including free thermal expansion and hygroscopic effects in addition to creep. When comparisons were made with the in-cartridge creep specifications shown in Table IV, MP-PET and ME-Aramid appear to meet the requirements for future tapes based on viscoelastic creep strain with MP-PEN creep strains measured to be slightly above the specifications. However, higher humidity levels used for the in-cartridge creep specifications along with a slightly higher temperature would lead to higher creep strains for the tapes.

To account for tension, bending, and radial stresses when a tape is stored in a reel, circumferential and lateral creep strains were determined using the creep-compliance data. These lateral creep strains were determined for outer and inner wraps of a magnetic tape when it is stored in a reel. Creep-compliance information from TTS was used at 30 and 50°C reference temperatures. Lateral creep strains for the three tapes were found to be lower at the outer wrap than at the inner wrap at specific creep times, and longer creep times led to larger creep strains. There also appears to be a greater change in creep strain through the thickness of tape segments at inner wraps when compared with tape segments at outer wraps. If total creep response is considered, lateral creep strains determined for the polyester-based MP-PEN and MP-PET tapes stored in a reel meet requirements specified in Table III for 2007, whereas the ME-Aramid tape meets requirements specified for 2015. However, viscoelastic lateral creep strains calculated for the outer and inner wraps of all the tapes are below the requirements specified for 2015. When compared with in-cartridge creep specifications from PES measurements shown in Table IV, the viscoelastic lateral creep strains determined for MP-PET and ME-Aramid are below the specifications for future tapes, whereas the viscoelastic creep strains for MP-PEN are slightly higher than the specifications for future tapes. Limitations of the stress model along with higher humidity levels used for the in-cartridge creep experiments were discussed to account for the differences between the creep strains and specifications.

Using the creep-compliance data and calculated stresses for tape storage in a reel, creep strains could be predicted for future tapes with thinner, lower compliance coatings. Front coat thickness reduction led to a slight increase in creep strain, and a combined reduction in front coat and substrate thickness led to an even greater increase in creep strain. When tape compliance alone is reduced, creep strains are significantly reduced. The combined effect of thickness and compliance reduction also led to an overall reduction in creep strain, although this creep strain reduction was not as great as what could be achieved by reducing only the compliance. More substantial decreases in creep strain were predicted for the inner wrap when compared with the outer wrap.

Using a rule of mixtures method together with TTS, creep-compliances for the front coat and back coat of an MP-PEN tape were determined. The compliance of a front coat + substrate dual layer sample appeared to be higher and increase at a higher rate than the compliance of the substrate. This indicated that the front coat plays a more dominant role in the overall creep-compliance of the tape. The rule of mixtures method allowed the front coat compliance to be plotted as a separate data set, and the compliance of this layer increased significantly over a relatively short time period when compared with the substrate. It was also possible to determine a general increasing trend to the compliance for the back coat, but there was a great deal of variability to the data set. Using the creep-compliance information for the multiple layer tape, stresses in each layer could be determined through the thickness of the tape. In general, stresses in the front coat decreased as a function of creep time, whereas stresses in the substrate showed a slight increase. Inconsistent stress profiles could lead to loose wraps and lost information when the head tries to read information from the tape.

Additional information about creep recovery and shrinkage could be extracted from the data sets acquired for the creep experiments. Creep-recovery experiments showed that the MP-PEN and ME-Aramid materials recovered completely within a time period less than that used for the creep experiment. MP-PET, on the other hand, did not recover completely after

even greater time periods than the creep experiment. At the start of an experiment, shrinkage of the tapes could be measured for a 10 h time period. ME-Aramid tape showed the least amount of shrinkage, whereas ME-PEN showed the largest amount of shrinkage with MP-PET in between. Shrinkage appeared to be dominated by substrate characteristics as demonstrated for MP-PEN and its PEN substrate.

The author acknowledges the members of the INSIC Tape Program for their support and valuable input throughout the course of this research activity. The author also thanks Ric Bradshaw of IBM for providing the tape, substrate, and dual-layer thickness measurements needed to study the creep characteristics of magnetic tape layers.

References

1. International Magnetic Tape Storage Roadmap; Information Storage Industry Consortium: San Diego, CA, April 2005.
2. Jaquette, G. A. IBM J Res Dev 2003, 47, 429.
3. Weick, B. L.; Bhushan, B. J Appl Polym Sci 1995, 58, 2381.
4. Weick, B. L.; Bhushan, B. J Inf Stor Proc Syst 2000, 2, 1.
5. Weick, B. L.; Bhushan, B. J Appl Polym Sci 2001, 81, 1142.
6. Higashioji, T.; Bhushan, B. J Appl Polym Sci 2002, 84, 1477.
7. Ma, T.; Bhushan, B. J Appl Polym Sci 2003, 89, 3052.
8. Bhushan, B. Tribology and Mechanics of Magnetic Storage Devices, 2nd ed.; Springer-Verlag: New York, 1996.
9. Bhushan, B. Mechanics and Reliability of Flexible Magnetic Media, 2nd ed.; Springer-Verlag: New York, 2000.
10. Ferry, J. D. Viscoelastic Properties of Polymers, 3rd ed.; Wiley: New York, 1980.
11. Tschoegl, N. W. The Phenomenological Theory of Linear Viscoelastic Behavior: An Introduction; Springer-Verlag: New York, 1989.
12. Aklonis, J. J.; MacKnight, W. J. Introduction to Polymer Viscoelasticity; Wiley: New York, 1983.
13. Press, W. H.; Flannery, B. P.; Teukolsky, S. A.; Vetterling, W. T. Numerical Recipes in C: The Art of Scientific Computing; Cambridge University Press: New York, 1988.
14. Williams, M. L.; Landel, R. F.; Ferry, J. D. J Am Chem Soc 1955, 77, 3701.
15. Lin, L. Y.; Westmann, R. A. ASME J Appl Mech 1989, 56, 821.
16. Lee, Y. M.; Wickert, J. A. ASME J Appl Mech 2002, 69, 358.
17. Lee, Y. M.; Wickert, J. A. ASME J Appl Mech 2002, 69, 130.
18. Jones, R. M. Mechanics of Composite Materials, 2nd ed.; Taylor & Francis: Philadelphia, 1999.
19. Weick, B. L.; Bhushan, B. IEEE Trans Magn 1995, 31, 2937.